Since January 2020 Elsevier has created a COVID-19 resource centre with free information in English and Mandarin on the novel coronavirus COVID-19. The COVID-19 resource centre is hosted on Elsevier Connect, the company's public news and information website.

Elsevier hereby grants permission to make all its COVID-19-related research that is available on the COVID-19 resource centre - including this research content - immediately available in PubMed Central and other publicly funded repositories, such as the WHO COVID database with rights for unrestricted research re-use and analyses in any form or by any means with acknowledgement of the original source. These permissions are granted for free by Elsevier for as long as the COVID-19 resource centre remains active.

Analytica Chimica Acta 1234 (2022) 340297

Contents lists available at ScienceDirect

Analytica Chimica Acta

journal homepage: www.elsevier.com/locate/aca

Recent advances in airborne pathogen detection using optical and electrochemical biosensors

Rajamanickam Sivakumar, Nae Yoon Lee *

Department of BioNano Technology, Gachon University, 1342 Seongnam-daero, Sujeong-gu, Seongnam-si, Gyeonggi-do, 13120, South Korea

HIGHLIGHTS

- Conventional techniques involved in airborne pathogen detection are discussed.
- Emerging optical biosensors for airborne pathogen detection are summarized.
- The electrochemical biosensors for airborne pathogen detection are described.
- The pros and cons of the optical and electrochemical biosensors are explained.

GRAPHICAL ABSTRACT

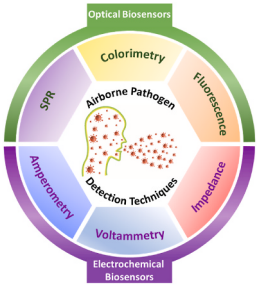

ARTICLE INFO

Keywords:
Infectious disease
Point of care test
Transducer
Visual inspection
Electrical signal

ABSTRACT

The world is currently facing an adverse condition due to the pandemic of airborne pathogen SARS-CoV-2. Prevention is better than cure; thus, the rapid detection of airborne pathogens is necessary because it can reduce outbreaks and save many lives. Considering the immense role of diverse detection techniques for airborne pathogens, proper summarization of these techniques would be beneficial for humans. Hence, this review explores and summarizes emerging techniques, such as optical and electrochemical biosensors used for detecting airborne bacteria (*Bacillus anthracis*, *Mycobacterium tuberculosis*, *Staphylococcus aureus*, and *Streptococcus pneumoniae*) and viruses (Influenza A, Avian influenza, Norovirus, and SARS-CoV-2). Significantly, the first section briefly focuses on various diagnostic modalities applied toward airborne pathogen detection. Next, the fabricated optical biosensors using various transducer materials involved in colorimetric and fluorescence strategies for infectious pathogen detection are extensively discussed. The third section is well documented based on electrochemical biosensors for airborne pathogen detection by differential pulse voltammetry, cyclic voltammetry, square-wave voltammetry, amperometry, and impedance spectroscopy. The unique pros and cons of these modalities and their future perspectives are addressed in the fourth and fifth sections. Overall, this review inspected 171 research articles published in the last decade and persuaded the importance of optical and electrochemical biosensors for airborne pathogen detection.

* Corresponding author.
E-mail address: nylee@gachon.ac.kr (N.Y. Lee).

https://doi.org/10.1016/j.aca.2022.340297
Received 20 April 2022; Received in revised form 27 July 2022; Accepted 18 August 2022
Available online 23 August 2022
0003-2670/© 2022 Elsevier B.V. All rights reserved.

1. Introduction

Airborne pathogens, such as bacteria (e.g., *Mycobacterium tuberculosis*), viruses (e.g., Influenza), and fungi (e.g., *Aspergillus niger*), easily enter living organisms either directly by breathing or indirectly by settling onto surfaces, creating a severe threat to human health and economic growth [1–3]. Currently, the world is facing an adverse condition due to the pandemic of airborne SARS-CoV-2, producing more than 178 million confirmed victims, including 3.8 million deaths, reported to the World Health Organization (WHO) as of June 2021. Thus, a rapid diagnosis of infectious pathogens is necessary to reduce or prevent the pathogen transmission rate within humans [4–6]. The point of care test (POCT) is potentially involved for infectious disease detection, and WHO has set the ASSURED criteria for designing an ideal POCT platform (**a**ffordable, **s**ensitive, **s**pecific, **u**ser-friendly, **r**apid, **e**quipment-free, and **d**eliverable) [4,7,8].

Several techniques, such as culture, microscopy, immunoassays, and molecular diagnostics, have enormously contributed to infectious disease identification [7,9–11]. Although the culture-based method is one of the best techniques for pathogen detection, the complicated procedure, long time to procure results, and requiring well-trained professionals hinder further applications. Similarly, low magnification microscopy cannot detect pathogens effectively; thus, these methods are not as prevalent as POCT for infectious disease detection [10]. Typically, reverse transcriptase (RT) polymerase chain reaction (PCR) (RT-PCR) and enzyme-linked immunosorbent assay (ELISA)-based methods are widely used for infectious virus detection [12,13]. However, the ELISA technique faces severe issues due to expensive antibodies and more detection time [14]. RT-PCR provides high sensitivity and specificity for detecting pathogens. However, considering the costly analytical equipment and additional purification step, the RT-PCR technique is not robust [12]. Because of user-friendliness, affordability, and rapidity, optical and electrochemical biosensors have recently provided sufficient space for airborne pathogen detection [6,15–17].

In view of selectivity, cost-effectiveness, and detection easily judged by the naked eye, optical biosensors are popular using surface plasmon resonance (SPR), colorimetry, and fluorescence strategies for airborne pathogen detection [18–20]. Only a few nanomaterials (NMs) have an SPR property and exclusively interact with pathogens, developing an instantaneous light signal on their surface that can be seen by the naked eye [5,6]. Noble metals, such as gold (Au) and silver (Ag) nanoparticles (NPs), have unique SPR properties, effectively participating in the detection process [7,21]. Nanozymes are artificial enzymes with unique features, such as easy handling, high stability, and feasible synthetic methodology. Thus, it has been used instead of enzymes in the colorimetric process as a signal transducer for pathogen detection [22]. Currently, metal-organic frameworks (MOFs), Au/Pt NPs, magnetic NPs (MNPs), and carbon nanotubes (CNTs)/Au nanohybrids function as nanozymes for oxidating peroxidase substrates, developing distinguishable color in the presence of airborne bacteria and viruses [19,23–25]. Furthermore, other methods, such as molecular methods, and G-quadruplex DNAzyme, were used in identifying pathogens in the colorimetric platform [26–29]. Recently, the fluorescence method has drawn attention to pathogen detection due to its fast response, high signal-to-volume ratio, simple fabrication, and economical [20,30]. Fluorescent sensor materials only emitted photons when binding with genomic target analytes; thus, it is convenient for identifying pathogens [31]. Furthermore, this technique has higher sensitivity than microscopy or immunoassay-based methods [10,11].

Various features, such as high sensitivity, ease of fabrication, and portability are taken into the account to construct the POCT, and the electrochemical biosensor almost satisfies these criteria. Thus, it is proficiently used in detecting airborne pathogens [2,14]. Electrochemical biosensors read various electrical signals, such as current, resistance, potential, and impedance format, generated through the interaction between the transducer and biomolecules. The transducer is a working electrode modified with proteins or antibodies to detect target analytes [32,33]. The electrical signals produced in the presence of airborne pathogens were measured through various techniques, such as voltammetry (cyclic voltammetry (CV), square-wave voltammetry (SWV), differential pulse voltammetry (DPV)), amperometry, and electrochemical impedance spectroscopy (EIS) [34–38]. Because of the numerous techniques employed in the electrochemical biosensor, it has been efficiently applied in disease monitoring and medical diagnosis [14]. Based on the applications of the optical and electrochemical biosensors, a comparison of these methods with other techniques is shown in Table 1. Despite numerous articles published in recent times towards airborne pathogen detection, limited review articles are available [4,6]. Even the published review articles did not provide adequate detection strategies for airborne bacteria and viruses. Hence, this review focuses on airborne bacteria and virus detection based on emerging techniques, such as optical and electrochemical biosensors (Fig. 1). Specifically, SPR, colorimetry, and fluorescence techniques used in the optical biosensors for infectious pathogen detection are discussed. The electrical signals generated in the presence of airborne pathogens were measured using DPV, CV, SWV, amperometry, and EIS are discussed. Finally, a conclusion and future perspectives are provided for certifying the credibility of this review. In addition, the exponential growth of relative publications on optical and electrochemical biosensors for airborne pathogen detection is shown in Fig. 2.

2. Optical biosensors for airborne pathogen detection

Pathogens, such as bacteria, viruses, fungi, and protozoa, are prevalent in developing pandemic situations. Because of their severity, bacteria and viruses create more diseases worldwide [1,6]. Significantly, these pathogens can be detected rapidly and on-site using optical biosensors. This section extensively evaluates SPR, colorimetric, and fluorescence-based biosensors. Tables 2 and 3 show a detailed comparison study based on optical biosensors for airborne bacteria and virus detection.

Table 1
Comparison of the optical and electrochemical biosensors with other techniques.

Detection methods	Advantages	Disadvantages
Optical biosensors	● Real-time detection ● Point of care test ● High sensitivity ● short detection time	● Highly sensitive ● Low compatibility ● Low reproducibility
Electrochemical biosensors	● Robustness ● Portable ● Excellent detection limits	● Sensitive to sample matrix ● Low selectivity ● Need of trained specialists
Mass-based biosensors	● High sensitivity ● Rapid ● Stable output	● Low sensitivity ● Interference induces by nonspecific binding
Culture methods	● Affordable ● Less equipment usage ● High selectivity	● Low sensitivity ● Time-consuming process ● Hard to culture some microorganism ● Biosafety issues
Molecular methods	● High throughput ● High selectivity ● High specificity	● Expensive process ● Complex procedure ● Professional equipment needed
Gene Sequencing	● Good stability ● High selectivity ● High accuracy	● Laborious ● Time-consuming process ● High measurement cost

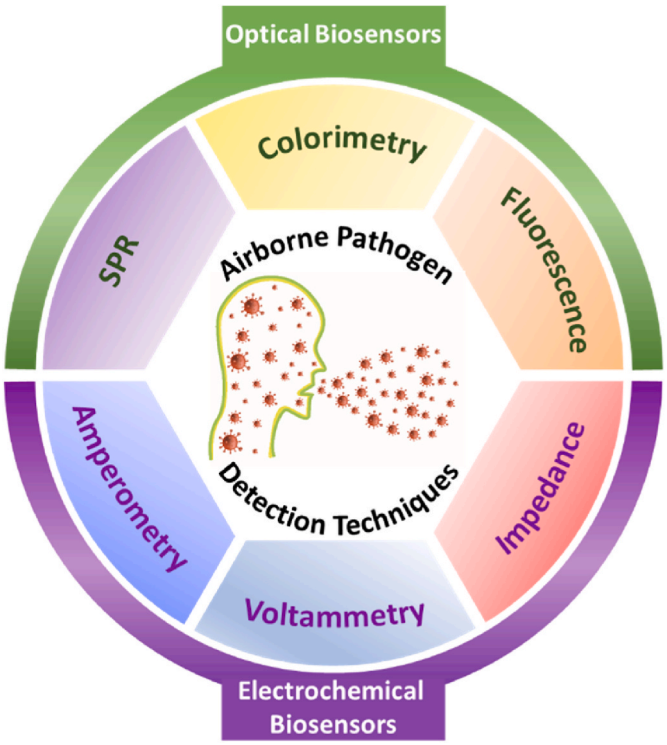

Fig. 1. Schematic diagram showing optical and electrochemical biosensors following various mechanisms for airborne pathogen detection.

2.1. Airborne bacteria detection

Airborne bacteria, specifically *Bacillus anthracis, Mycobacterium tuberculosis, Staphylococcus aureus,* and *Streptococcus pneumoniae* widely affect humans, and detecting them using optical biosensors is discussed here.

2.1.1. Bacillus anthracis (B. anthracis) detection

2.1.1.1. Colorimetry strategy. *B. anthracis* is harmful spore-forming bacteria, that develops a contagious disease called anthrax. Unfortunately, *B. anthracis* spores endure harsh conditions, such as high temperatures, drought, and ultraviolet (UV) light, and even continuously germinate after the bacteria is dead [39]. Because of the high toxicity and rapid transmission, *B. anthracis* spores are considered biological weapons and must be monitored through modern techniques to prevent disease outbreaks [40,41]. Dipicolinic acid (DPA), a typical biomarker, presents in dry spores (5%–15%) and maintains the stability of bacterial DNA [42]. Thus, the rapid and facile detection of biomarker DPA identifies bacteria because it constitutes a certain percentage in *B. anthracis* spores. In general, AgNPs actively participate in detecting pathogens based on their unique SPR property [21]. The yellow color of AgNPs is aggregated while producing a complex with europium ion (Eu^{3+}) and the color changes to pink. DPA has excellent coordination ability with Eu^{3+}, which helps disperse AgNPs from the Ag–Eu^{3+} complex and retains their original yellow color. Using this SPR phenomenon, the limit of detection (LOD) of *B. anthracis* in the real sample was measured as 0.31 μM [43]. Significantly, this process has detected the DPA using colorimetry as well as fluorescence methods. These dual-mode strategies can assist to confirm the consistency and accuracy of the detection results. Moreover, the ratiometric colorimetric assay has two wavelengths that could exhibit excellent accuracy toward target analytes detection compared with the measurements achieved at a single wavelength. Hence, this process utilized the ratiometric colorimetric method. Furthermore, in the nano complexes, AgNPs act as a "nano-quencher" which can induce the fluorescence of Eu^{3+}, and thus 7.5 μM of DPA was easily perceived by the naked eye. In addition, the Ag–Eu^{3+} complex has an almost similar sensitivity for DPA detection compared with other lanthanide upconversion NPs (UCNPs)-based nanosensors [44].

The anthrax protective antigen (PA_{83}) is another biomarker for *B. anthracis*, detected using the sandwich immunoassay-based technique. The AuNPs-attached antibodies (Abs) were linked to the PA_{83} to produce the sandwich immunosensor (Abs–PA_{83}–Abs–AuNP). Then, the

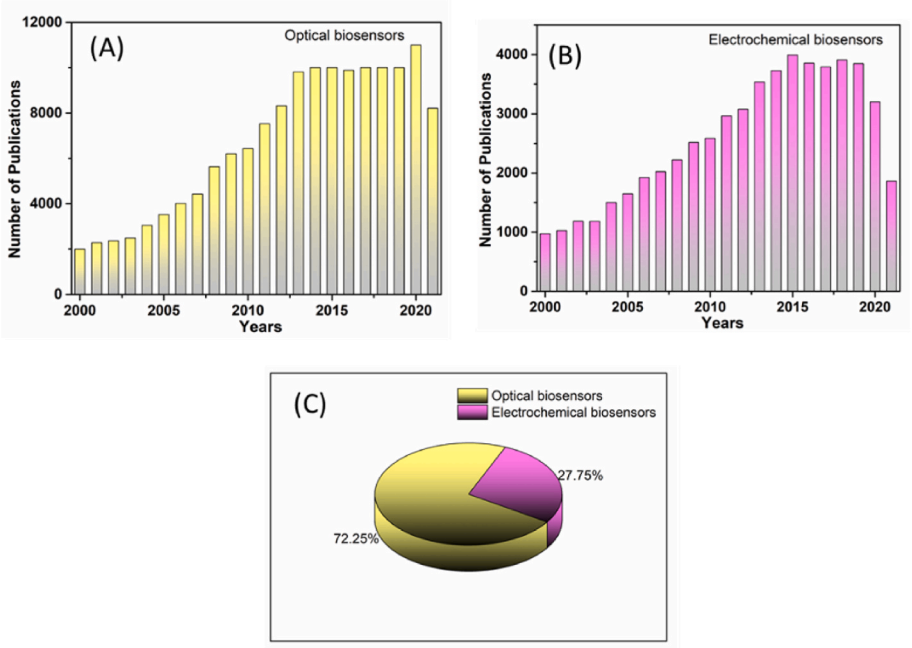

Fig. 2. The charts display the total number of publications per year towards airborne pathogen detection using (A) optical biosensors, (B) electrochemical biosensors, and (C) overall contribution of optical and electrochemical biosensors for airborne pathogen detection. (Data collected from the scifinder-n.cas.org on January 01, 2022, using "colorimetric biosensors", "electrochemical biosensors", and "airborne pathogen" as keywords).

Table 2
A detailed comparison of the optical biosensor for airborne bacteria detection.

Target bacteria	Detection method	Conjugate materials	Linear range	LOD	Time (min)	Real sample	Ref
B. anthracis	SPR	AgNP	1.0–25 μM	0.31 μM	5	Lake water	43
	Colorimetry	UCNPs−TPP/EBT	2–200 μM	0.9 μM	60	Human serum	44
		Pt/AuNP	–	1 nM	20	–	23
		LAMP primers		500 fg	60	–	47
	Fluorescence	Tb/Eu(MOF)	50–700 nM	4.55 nM	<2	Human serum	48
		Tb/Eu@bio-MOF		34 nM	4	Human serum	50
		R6H/Eu(MOF)	0–80 μM	4.5 μM	–	–	51
		RSPh/Eu(MOF)	–	0.52 μM	<1	–	52
		Si NP/Tb-MOFs	0.025–3 μM	5.3 nM	<1	Bovine serum albumin (BSA)	53
		R6H/EDTA-Eu	10−50 nM	10 nM	–	–	54
		Tb–P/CPs	0−8 μM	5 nM	<1	Urine	40
		Eu/ZnO QD	0−4 μM	3 nM	–	–	39
		Eu/Si QD	0−35 μM	1.02 μM	–	–	56
		Eu/EBT-CD	0.1–12 μM	10.6 nM	10	Urine	57
M. tuberculosis	SPR	AuNP	–	1.25 pM	15	–	59
		AuNP	0–100 ng mL^{-1}	1.56 ng mL^{-1}	90	Urine	60
	Colorimetry	LAMP primers	–	5 pg mL^{-1}	60	–	26
	Fluorescence	MNP	–	10^2 CFU mL^{-1}	30	Human saliva	62
S. aureus	SPR	AuNP	–	19 CFU mL^{-1}	30	Water	64
		AuNP	5–40 ng μL^{-1}	8.73 ng μL^{-1}	15	–	65
		Labeled AuNP	–	0.02 μM	5	Ocean water	66
		Au/Ag NR	–	25 CFU mL^{-1}	20	Milk	21
	Colorimetry	Au/Fe_3O_4 NP	10–10^6 CFU mL^{-1}	10 CFU mL^{-1}	12	Milk	68
		AgNC	10–10^6 CFU mL^{-1}	4.9 CFU mL^{-1}	5	–	71
		MNP	10–10^8 CFU mL^{-1}	3 CFU mL^{-1}	<1	Milk	72
	Fluorescence	NBD–Cl	–	1 CFU mL^{-1}	15	Milk	73
		CuNC	10–10^8 CFU mL^{-1}	80 CFU mL^{-1}	45	Milk	74
S. pneumoniae	Colorimetry	G-quadruplex/hemin	–	156 CFU mL^{-1}	40	–	76
		LAMP primers	–	25 fg μL^{-1}	2	Blood	77
		LAMP primers	2 ng–2 fg μL^{-1}	20 fg μL^{-1}	–	–	8
	Fluorescence	GO		15 CFU mL^{-1}	30	–	30

Table 3
A detailed comparison of the optical biosensor for airborne virus detection.

Target virus	Detection method	Conjugate materials	Linear range	LOD	Time (min)	Real sample	Ref
Influenza A (H3N2 subtype)	SPR	ConA/GOx/AuNP	0–200 μg mL^{-1}	11.1 μg mL^{-1}	20	–	79
		AuNP	–	7.8 HAU	30	–	18
	Colorimetry	AuNPs/CNTs	–	3.4 PFU mL^{-1}	10	Human serum	25
	Fluorescence	MbO_3/g-CN QD	45–250 PFU mL^{-1}	45 PFU mL^{-1}	5	Human serum	85
H1N1 subtype	Colorimetry	AuNP	–	10 pg mL^{-1}	<1	Human serum	81
		PDA vesicles		10^5 PFU mL^{-1}	–	–	82
		RT-LAMP primers		3×10^{-4} HAU	40	–	84
Avian influenza A (H7N9 subtype)	SPR	AuNP	5–50 pg mL^{-1}	1.25 pg mL^{-1}	10	Human serum	87
	Fluorescence	FMNP	–	0.02 pg mL^{-1}	30	Chicken serum	90
H5N1 subtype	SPR	AuNBP	1–2.5 ng mL^{-1}	1 pg mL^{-1}	35	Human serum	88
	Colorimetry	RCA primers	0.16–1.20 pM	28 fM	–	–	27
H9N2 subtype	Fluorescence	FMNP	300–900 ng mL^{-1}	69.8 ng mL^{-1}	30	Chicken lung	91
		RuSiNP	25 pg–25 ng mL^{-1}	14 fg mL^{-1}	30	Chicken liver	92
Norovirus	SPR	AuNP	10–53 PFU mL^{-1}	10 PFU mL^{-1}	–	BSA	69
	Colorimetry	Graphene/AuNP	–	92.7 pg mL^{-1}	10	Human serum	97
		V_2O_5	1 pg–100 ng mL^{-1}	0.34 pg mL^{-1}	1	Human serum	98
		Au/AgNP	–	10.8 pg mL^{-1}	–	–	95
	Fluorescence	GO/6-FAM	13 μg–13 ng mL^{-1}	3.3 ng mL^{-1}	5	BSA	99
		AuNPs/CdSeS QDs	1 pg–5 ng mL^{-1}	0.48 pg mL^{-1}	5	Human serum	100
		AgNC	1.8 μM–20 nM	18 nM	–	–	101
SARS-CoV-2	SPR	AuNP	10 pM–100 nM	1 copy	30	Saliva	28
	Colorimetry	ASO/AuNP	0.2–3 ng μL^{-1}	0.18 ng μL^{-1}	10	BSA	106
	Fluorescence	Co-Fe@hemin	0.2–100 ng mL^{-1}	0.1 ng mL^{-1}	16	–	110

platinum (Pt) NPs were stabilized on the surface of the Abs–PA_{83}–Abs–AuNP biosensor, which oxidized the 3,3′,5,5′–tetramethylbenzidine (TMB) in the presence of hydrogen peroxide (H_2O_2) and produced blue color. Using this method, up to 1 nM of PA_{83} was detected within 2 min [23]. This colorimetric assay is more improved than other lateral-flow immunochromatographic assays (LFIA), where various transducers, such as horseradish peroxidase (HRP) and magnetic NPs are used [45,46].

2.1.1.2. Fluorescence strategy. The fluorescence-based strategy has contributed to infectious *B. anthracis* detection by means of detecting the biomarker DPA [39]. Lanthanide (Ln), such as terbium (Tb) and Eu, was incorporated into the MOF to produce a Tb/Eu(MOF) sensor, sending a ratiometric fluorescent signal for identifying the DPA [48]. Tb/Eu(MOF) sensor exhibited red-orange emissions due to the energy transfer from Tb^{3+} to Eu^{3+} in the system. Substantially, the DPA has more affinity with Tb^{3+}, restricting the energy transfer between the lanthanides, showing a consequent yellow-green emission. Notably, 60 mM of *B. anthracis* spores can be acceptable for humans according to WHO [49]. However, this method has detected DPA up to 4.55 nM, revealing its significance

[48]. This method has established a ratiometric self-calibrating MOF sensor by incorporating two lanthanides that did not demand any external instrument for specific calibration. Significantly, the DPA was sensed within 20 s due to the strong interaction between the DPA and Tb, revealing that the lanthanide-MOF sensor will be beneficial for detecting the DPA in biological samples rapidly. More importantly, this process has outstanding specificity toward DPA, providing a precise method for detecting DPA in complex biological samples.

The chitosan-based fluorescent biosensor has been involved in DPA detection due to its simple functionalization and biocompatibility. In the chitosan backbone, the R6H and EDTA were effectively attached, and Eu^{3+} particularly produced a complex with EDTA [54]. The fabricated R6H/EDTA–Eu^{3+} biosensor detected DPA up to 10 nM (Fig. 3) which revealed higher sensitivity than the adenine-attached Ln/bio-MOF [50]. Lanthanide phosphonate coordination polymers (Ln–P/CPs) have several unique features, such as large stoke shifts, excellent emissions, and highly stable fluorescence which are induced Ln-P/CPs to perform in the DPA detection [55]. Significantly, the Tb–P/CPs fluorescence intensity gradually increased when increasing DPA from 0 to 8 μM [40]. The LOD was 5 nM and showed higher sensitivity than the NP-based colorimetric method [44]. Due to the high affinity of lanthanides with DPA, various groups have developed the Eu^{3+} functionalized quantum dots (QDs) for *B. anthracis* detection. Zhou et al. fabricated Eu^{3+}/ZnO QDs, where Eu^{3+} was employed as a signal transducer, and ZnO QDs functioned as an internal reference. In this method, the detection process was completed within 8 s due to the large surface area of the ZnO QDs, increasing the contact with DPA [39]. This process was detected as low as 3 nM and exhibited higher sensitivity than other methods [51,52].

2.1.2. *Mycobacterium tuberculosis (MTB)*

Globally, an estimated 10 million people were affected by MTB in 2019 and 1.2 million were confirmed dead, according to the WHO report. Due to the seriousness of MTB, "early diagnosis and early treatment" is the most effective way to control it and save humans [58].

2.1.2.1. Colorimetry strategy. The SPR-based colorimetric biosensor has been designed for detecting ESAT-6 protein present in MTB. In the process, ESAT-6 was immobilized on specific antibodies, and AuNPs were added to it. The red color of the ESAT-6-contained biosensor changed to blue color due to the salt-induced aggregation, and the LOD was measured up to 1.25 pM [59]. Similarly, another antigen, namely, MTB antigen 85B (Ag85B), was detected using AuNPs in the immunoblotting technique. The recombinant GBP-50B14 fusion antibody was used to produce the immunoassay because it has a high affinity with Ag85B and AuNP. Based on the sustainability of the red color in the biosensor, up to 1.56 ng mL^{-1} Ag85B could be detected [60]. More importantly, this immunoblotting technique is also capable of detecting another antigen CFB10 of MTB. Furthermore, the sensitivities of Ag85B and CFP10 were 90.5% and 76.2%, respectively, showing higher sensitivity than the ELISA [61]. Hence, detecting these biomarkers using the immunoblotting technique with higher sensitivity can diagnose TB at an early stage.

2.1.2.2. Fluorescence strategy. MTB is pathogenic and has slow growth in the culture medium. Hence, to avoid handling MTB for the experiment, *Mycobacterium smegmatis (M. smegmatis)* can be used because it has a similar physiological property as MTB and is nonpathogenic. *M. smegmatis* was functionalized with MNPs for facile magnetic separation, and the progeny mycobacteriophages were used to disrupt the *M. smegmatis* cells. The fluorescence developed in the system due to the release of intracellular adenosine triphosphate. Using this protocol, the LOD was 3.8×10^2 CFU mL^{-1} [62].

2.1.3. *Staphylococcus aureus (S. aureus)*

S. aureus has high pathogenicity and antibiotic resistance causing severe infections; therefore, it is one of the most common human pathogens, inevitably requiring robust analytical detection techniques [63].

2.1.3.1. Colorimetry strategy. The SPR property of AuNPs is significant to identify *S. aureus*. For instance, a combination of cysteamine (CS), *S. aureus*-specific pVIII fusion protein (fusion-pVIII), and AuNP have constructed a biosensor (CS/AuNP/fusion-pVIII) for *S. aureus* detection. In the presence of *S. aureus*, AuNPs were aggregated on its surface, changing the biosensor color from red to blue. Notably, this method has high specificity toward *S. aureus*, and the LOD was 19 CFU mL^{-1} [64]. In this study, the phage display technique was introduced to identify the fusion-pVIII. Indeed, the phage display technique can easily isolate the target protein without losing its activity. Significantly, the fabricated biosensor has shown high specificity due to the strong interaction

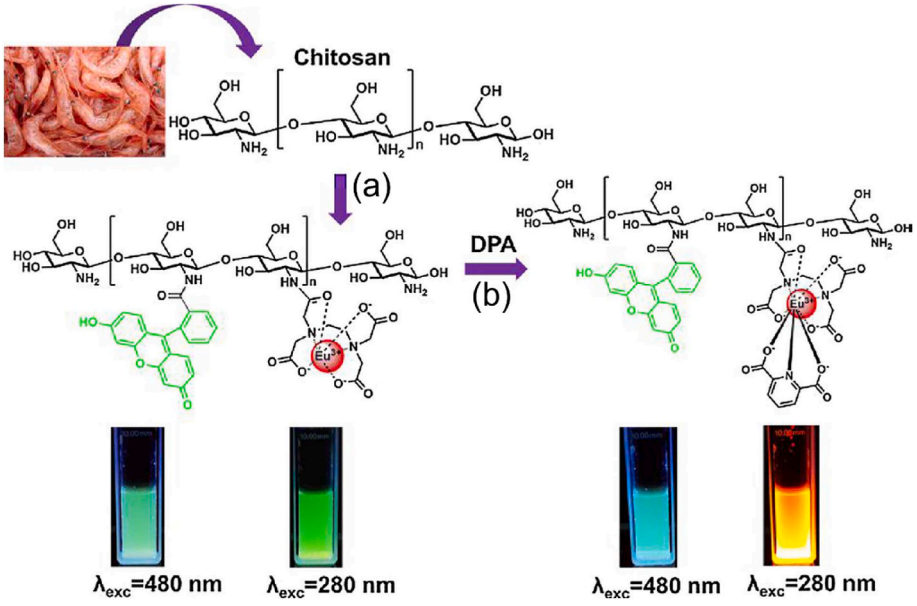

Fig. 3. Schematic illustration of fluorescence-sensing platform for anthrax biomarker (DPA) detection. (a) Fabrication of R6H derivative-based fluorescent probe using chitosan and EDTA–Eu^{3+} complex. (b) The gradual increase of the probe's emission upon the addition of DPA. Reproduced from the published article [54].

between the fusion-pVIII and *S. aureus*. Moreover, the biosensor recovery in the real sample was in the range of 95–110%. Thus, this method could be utilized to monitor *S. aureus* in environmental samples efficiently [64]. Similarly, another AuNP aggregation-based detection process used inorganic salt for distinguishing positive and negative samples. In the process, the single-stranded DNA (ssDNA) attached to the AuNPs, hybridized with *S. aureus* DNA, sustaining the red color in it. However, it turned blue when adding sodium chloride (NaCl). Using this method, 8.73 ng μL^{-1} *S. aureus* can be detected (Fig. 4a) [65].

Another promising method has proposed an MNP/DNA/alkaline phosphatase (ALP)-based biosensor for monitoring the *S. aureus* concentration. When adding *S. aureus*, the ALP was released from the biosensor due to the characteristic behavior of naturally secreted MNase [66]. The released ALP converts the L-ascorbic acid 2-phosphotrisodium salt to ascorbic acid which helps to produce the Ag nanoshell on the Au nanorods (AuNRs). Significantly, this method showed light green to red color, depending on the *S. aureus* concentration [21]. The detection of *S. aureus* using the modification of AuNPs with oligonucleotide is making the process more tedious and time-consuming [66]. However, in this method, the unlabelled AuNRs were involved in *S. aureus* detection, which confirmed its importance in pathogen detection. In addition, the formation of Au–Ag alloy NRs not only has significant benefits in terms of high sensitivity and detection time but also potential for semi-quantitative colorimetric pathogen detection due to producing a multicolor based on the *S. aureus* concentration.

In general, nanozymes have peroxidase-mimicking activities, which were used for *S. aureus* detection [67]. Zhang et al. synthesized the nanozymes using the composition of Au/Fe_3O_4 NPs, and it was functionalized with specific *S. aureus* aptamer *via* Au-sulfur interaction [68]. The aptamer-functionalized nanozymes' active sites were blocked when adding *S. aureus*, inhibiting the catalytic oxidation of TMB [19,69]. Thus, this method produced a lighter color in the presence of target bacteria, and the LOD was measured as 10 CFU mL^{-1} [68]. However, the RCA-based technique developed bright blue color by oxidizing TMB in the presence of *S. aureus* using an HRP catalyst. Essentially, the RCA method offered extreme sensitivity and selectivity for detecting *S. aureus*. Under optimum conditions, the RCA method potentially detects the target DNA up to 1.2 pM [70].

In terms of high surface area and more active sites, nanozymes produce a distinguishable color in the presence of bacteria. In fact, MNPs coated on the electrode surface were coupled with specific peptide sequences, displaying black color on the electrode surface. Furthermore, the peptide sequences in the electrode were cleaved when adding *S. aureus* protease and released MNPs. Consequently, the black color electrode surface changed to golden yellow color. More importantly, this biosensor detected the *S. aureus* within 1 min and has tremendous specificity against other bacteria [72]. Significantly, this process has performed both colorimetry as well as electrochemical approaches for *S. aureus* detection. Thus, the pathogen can be determined qualitatively and quantitatively which reveals the impact of this method. Typically, the utilization of expensive antibodies and aptamers is a time-consuming process. Hence, this technique employed nanozymes, and achieved the detection results within 1 min. Moreover, this method has been studied in both colorimetry and electrochemical approaches for *S. aureus* detection and thus it can be an ideal biosensor for on-site detection of infectious pathogens.

2.1.3.2. Fluorescence strategy. As with SPR and colorimetric-based techniques, the fluorescence method was also extensively employed

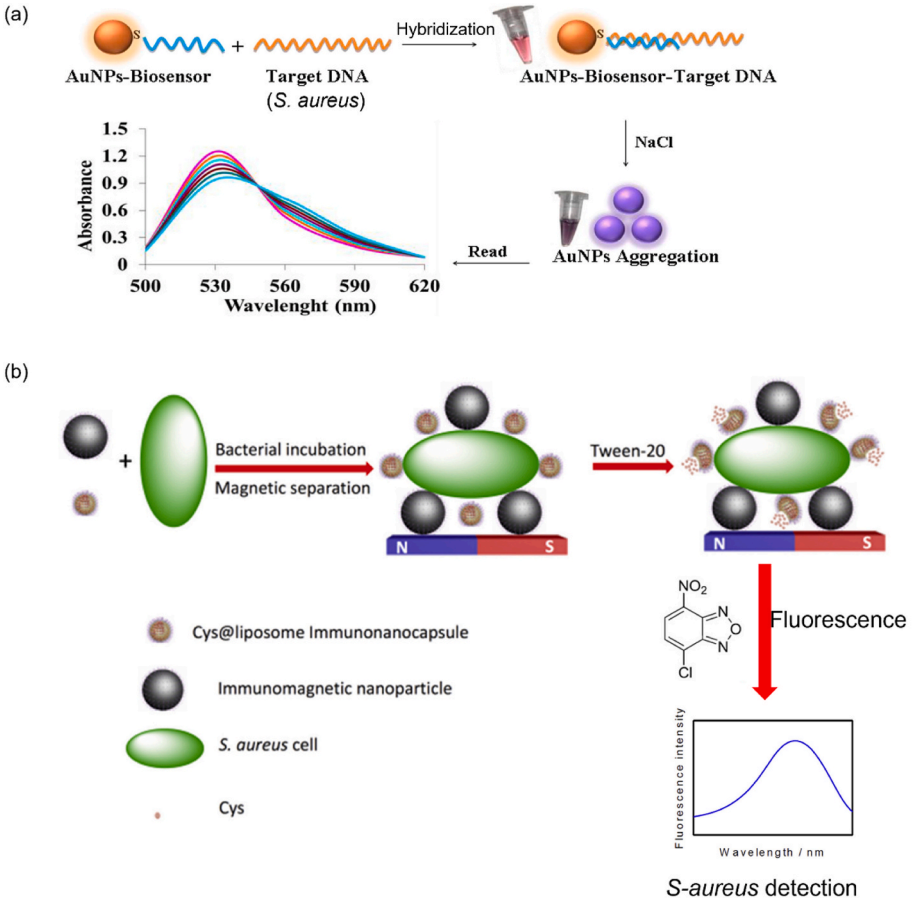

Fig. 4. (a) Schematic representation for naked-eye detection of *S. aureus* using AuNPs-probe. Reproduced from the published article [65]. **(b)** Schematic presentation of a fluorescent immunoassay for *S. aureus* detection. Reproduced from the published article [73].

for target bacteria detection. Deng et al. developed a fluorescent strategy for *S. aureus* detection using a novel reagent, namely, 4-chloro-7-nitrobenzo-2-oxa-1,3-diazole (NBD–Cl). In the process, synthesized cysteine (Cys)@liposome immuno-nanocapsules coupled with *S. aureus* cells and were destructed by Tween-20. Subsequently, Cys was released from the immunosensor, which reacted with NBD–Cl to generate the fluorescence signal. Using this fluorescent strategy, up to1 CFU mL^{-1} *S. aureus* was detected (Fig. 4b) [73]. Typically, copper NCs (CuNCs) have unique properties, such as nontoxicity, biocompatibility, and producing efficient fluorescence signals. Thus, CuNCs were attached with aptamer (apt) and antibiotics to produce a biosensor (apt/CuNCs/antibiotic) for quantifying *S. aureus* [74]. Interestingly, in the presence of *S. aureus*, CuNCs were aggregated, restricting the free movement of the molecules and producing bright fluorescence in the system. Based on the aggregation strategy, the LOD was 80 CFU mL^{-1}, a lower sensitivity than the AuNP-based aggregation method [64].

2.1.4. Streptococcus pneumoniae (S. pneumoniae)

S. pneumoniae is also known as pneumococcus, which mostly produces pneumonia and meningitis diseases. Furthermore, it is the fourth-largest microbial developing fatal infections, according to a WHO report. Hence, simple, rapid, and affordable analytical techniques are often the ideal choice for *S. pneumoniae* detection [75].

2.1.4.1. Colorimetry strategy. Recently, combining the catalyzed hairpin assembly (CHA) and signal transducer has been established colorimetric sensor for *S. pneumoniae* determination. Attaching the target DNA (*S. pneumoniae*) with hairpin DNA using the CHA process creates a new nucleic acid sequence with a high G-rich DNA content. The G-rich DNA in the presence of hemin produced a G-quadruplex/hemin complex, mimicking HRP activity, producing a distinguishable color. This colorimetric method detected *S. pneumoniae* at 156 CFU mL^{-1} [76]. Indeed, signal amplification is a significant process for pathogen detection. CHA can efficiently involve in signal amplification and has the advantage to overcome the drawback of enzymatic amplification. Thus, this technique adopted CHA for *S. pneumoniae* detection. However, it necessitates intricate engineering for modification with several analytes, which may limit this study to further clinical application.

2.1.4.2. Fluorescence strategy. Significantly, the fluorescence method was also lucrative for *S. pneumonia* detection. Therefore, a fluorophore-labeled aptamer (FL-apt) attached to target bacteria functions as a biosensor. Indeed, GO interacted with the aptamer via physisorption, reducing the fluorescent intensity of fluorophores through nonradiative excitation energy transfer [78]. Thus, FL-apt/*S. pneumoniae*-based biosensor gradually decreased their fluorescent intensity while increasing the concentration of GO and LOD was 15 CFU mL^{-1} [30].

2.2. Airborne virus detection

Viruses spreading through the air can cause serious illness and lead to death. Thus, detecting airborne viruses, such as influenza A (H1N1 and H3N2), avian influenza A (H5N1, H7N9, and H9N2), Norovirus, and SARS-CoV-2, are mandatory and optical biosensors involved in the detection process were discussed in this section [6].

2.2.1. Influenza A (H1N1 and H3N2)

H1N1 and H3N2 viruses have a high transmissibility rate, causing 670,000 deaths annually. Considering the resource-limited settings, identifying these viruses with the naked eye could be a high demand.

2.2.1.1. Colorimetry strategy. A sandwich biosensor (ConA/GOx/AuNP) has been developed using concanavalin A (ConA), glucose oxidase (GOx), and AuNPs for determining the H3N2 virus. The aptamer-functionalized H3N2 was combined with the ConA/GOx/AuNP biosensor, producing red color when the glucose solution was added to it. This method has high selectivity for H3N2 and was detected as low as 11.16 μg mL^{-1} [79]. In another method, AuNPs combined with CNTs function as nanozymes, oxidizing TMB in the presence of H3N2. This method was detected at 3.4 PFU mL^{-1}, which was 385 times more sensitive than the existing ELISA method (1312 PFU mL^{-1}) (Fig. 5a) [25]. Substantially, to synthesize the Au-CNT nanohybrid material, an environmentally friendly and inexpensive strategy was introduced in this technique as opposed to the existing methods which utilized harsh conditions for producing the Au-CNT nanohybrid [80]. Moreover, this technique has 500-fold higher sensitivity than commercial immunochromatography kits toward H3N2 detection.

AuNPs act as nanozymes that can be used instead of HRP to oxidize TMB in the presence of H_2O_2 to develop a colorimetric platform for H1N1 detection. This method simultaneously detects H1N1 and H3N2 with a limit of 10 pg mL^{-1} and 10 PFU mL^{-1}, respectively [81]. Indeed, although various nanomaterials have exhibited peroxidase-like activity, they are not easy to synthesize. Interestingly, this study utilized AuNP as nanozymes for pathogen detection due to its simple synthetic procedure. Therefore, the AuNP-based immunoassay method could be an useful alternative to other nanozyme-contained techniques for on-site clinical diagnostics [81]. Recently, a polydiacetylene (PDA)-based colorimetric method has been extensively employed for H1N1 detection [5]. The PDA vesicles have unique chromatic properties that were synthesized by photopolymerizing 10,12-pentacosadiynoic acid. Subsequently, the PDA vesicles were functionalized with specific peptide (PEP) sequences to make a PDA-PEP biosensor for capturing target pathogens. The PDA-PEP biosensor efficiently bound the H1N1 due to the high affinity of PEP to the HA protein of the influenza H1 strain. Furthermore, the blue color of the PDA-PEP biosensor changed to red color, and the LOD of this proposed method was 10^5 PFU mL^{-1} [82]. Another group followed the same strategy, in which polyvinylidene fluoride was used for immobilizing the PDA vesicles on its surface to produce a paper-like sensor, and smartphone technology was used to quantify the H1N1 [83].

2.2.2. Avian influenza A (AIV)

AIV can function as a gene donor, resulting in a higher death rate than other deadly viruses. Thus, prompt and essential analytical methods for early AIV diagnosis and restrain are needed [86].

2.2.2.1. Colorimetry strategy. The AuNPs/MNPs-based immunoassay was fabricated, in which ALP was attached to enhance the phosphate group's hydrolysis in the H7N9 backbone. Consequently, the AuNPs' color changed from red to blue when increasing the concentration of the target virus. Using this method, the LOD for H7N9 was measured as 1.25 pg mL^{-1} [87] (Fig. 5b). Another ALP strategy with SPR performance was used for H5N1 determination. The antigen-functionalized Au nanobipyramids (AuNBP) were combined with ALP, generating 4-aminophenol (4-AP) from the cleavage of the 4-aminophenyl phosphate. The produced 4-AP reduced the silver nitrate to AgNPs, which were deposited on the AuNBPs surface. Based on the silver deposition, bright colors were observed, and up to 1 pg mL^{-1} of H5N1 was detected. Typically, AuNBPs have higher sensitivity than the other nanostructures of the gold due to the high-index faceted on its edges. In addition, the AuNBP appears approximately at 750 nm (near-infrared region) in the UV–vis absorption spectrophotometer, and thus visual detection was easily perceived by the naked eye compared with other colorimetric methods. Owing to the formation of vivid colors, this approach may be employed for the semiquantitative detection of the H5N1 [88].

2.2.2.2. Fluorescence strategy. To perform multiplex detection, the fluorescence method is the easiest because different fluorescent emissions of target pathogens using a single light source can be collected simultaneously [89]. The immunoassay was fabricated using green, yellow, and red fluorescent MNPs (FMNPs) attached with the antibodies

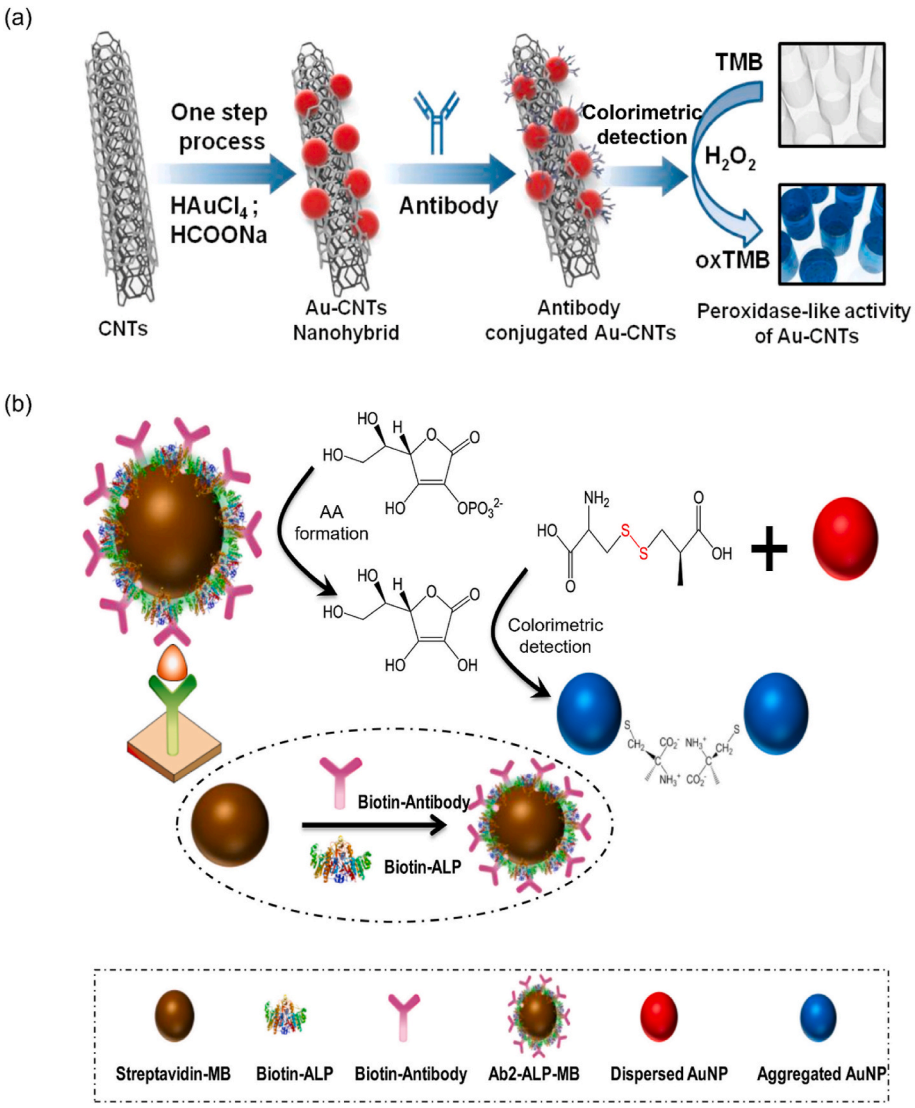

Fig. 5. (a) Schematic showing the detection of H3N2 virus based on the colorimetric peroxidase-like activity of Au-CNTs. Reproduced from the published article [25]. (b) The AuNPs/MBs-based immunoassay for the colorimetric detection of H7N9. Reproduced from the published article [87].

of target viruses, such as H9N2, H1N1, and H7N9 [90]. In the UV environment, the LOD of target viruses was 0.02 pg mL^{-1}, exhibiting higher performance than colorimetric methods [86,87]. The formation of hydrogels based on the hybridization between the aptamer and ssDNA was competently used for H5N1 detection. Noteworthy, the aptamer and ssDNA-produced hydrogel remained shrunk in the absence of the target virus. However, when the aptamer in the hydrogel interacts with H5N1, the hydrogel swells. Consequently, the aptamer quencher was released from the hydrogel, producing fluorescence, and this technique could detect 0.4 HAU of H5N1 [20]. In this study, the hydrogel-based aptasensor was introduced which has various advantages such as ease of synthesis, biocompatibility, high chemical stability, simple controllable modification, and low cost. Therefore, the label-free and hydrogel-based fluorescence aptasensor could be an alternative to expensive antibody/antigen-based immunosensors for pathogen detection.

2.2.3. Norovirus (NoV)

NoV is the most ubiquitous pathogen causing diverse diseases, such as diarrhea, food poisoning, and acute gastroenteritis in humans. It can survive any environmental conditions and is transmitted through direct contact, contamination of water, and aerosols [93]. Therefore, earlier diagnosis is preferred to prevent a contagious environment [94,95].

2.2.3.1. Colorimetry strategy. Lactoferrin (LF) is a common recognition molecule, as it attracts any virus in the sample; thus, LF-immobilized cotton swaps have been designed for NoV detection. The NoV was sandwiched between the antibody-conjugated AuNPs and LF-immobilized cotton swaps. The red color was sustained in the cotton swab even after washing with a phosphate-buffered saline solution. This developed immunoassay's LOD for NoV was measured between 10 and 53 PFU mL^{-1} [96]. Nanozymes, specifically nanohybrid, such as graphene-AuNPs, have intrinsic peroxidase-like properties that were preferentially used for detecting NoV-like particles (NoV-LPs). As using nanozymes for influenza virus detection [25,81], the antibody-attached graphene-AuNPs (nanozymes) adsorbed the NoV-LPs, oxidizing TMB in the presence of H_2O_2 and produced blue color. Remarkably, the LOD of this method was 92.7 pg mL^{-1}, which was 112 times lower sensitivity than the ELISA, and 41 times higher performance than the commercial kit [97]. Recently, vanadium oxide (V_2O_5) NP-encapsulated liposomes produced an immunoassay with NoV [98]. When liposomes break from the sandwich structure, the V_2O_5 NP is released, oxidizing the TMB. The LOD of this colorimetric method was 0.34 pg mL^{-1} (Fig. 6a). Interestingly, the released V_2O_5 NPs from captured liposomes not only have peroxidase-like activity but also acted as an electrochemical redox indicator. Therefore, this study has reported colorimetry as well as

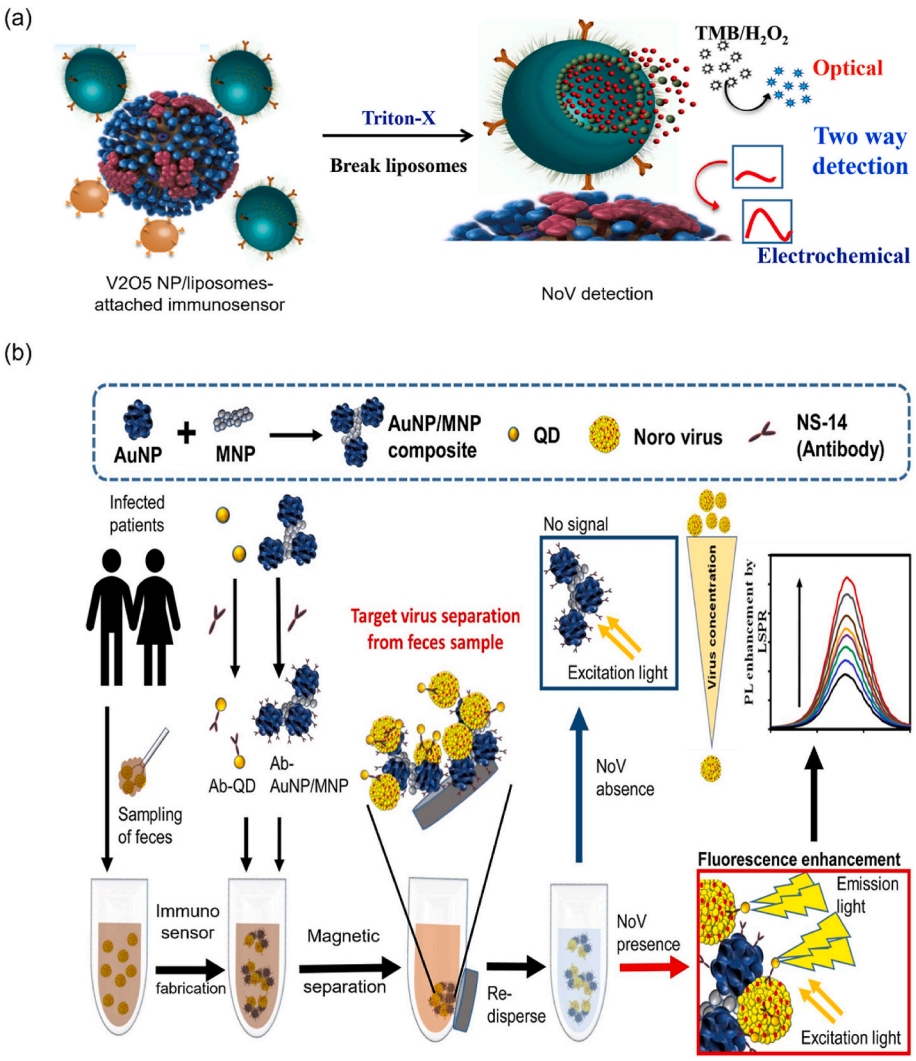

Fig. 6. (a) Detection of the NoV-based on the effective peroxidase-like activity using the release of V_2O_5 NPs from the captured liposomes. Reproduced from the published article [98]. (b) Schematic showing AuNP/MNP–NC–based sandwich immunoassay for NoV detection using the fluorescence strategy. Reproduced from the published article [100].

electrochemical approaches for NoV detection. Furthermore, the 1000-fold higher sensitivity is attained exhibiting the importance of the V_2O_5 NP-encapsulated liposome-based sensor. Also, the fabricated biosensor can be stored for 3 weeks without losing its catalytic activity, showing the remarkable stability of the sensor. Overall, the V_2O_5 NP-encapsulated dual-mode sensor avoids the intricated sample preparation and constraints the use of expensive instruments which makes the detection process facile and rapid [98].

2.2.3.2. Fluorescence strategy. To consider developing new techniques, cheap and convenient detection strategies must be developed. Hence, fluorescence-based techniques could fulfill the criteria for target virus detection [89]. The 6-carboxyfluorescein (6-FAM) attached with NoV-specific aptamer and its fluorescence was quenched while adding GO. When introducing the target NoV, the biosensor displayed strong fluorescence due to breakage between the aptamer and GO. Moreover, this fluorescence strategy showed a good linear range between 13 ng mL^{-1} and 13 μg mL^{-1} of NoV [99]. The synthesized NCs on the combination of AuNP and MNPs were producing a sandwich immunoassay when attached with a specific antibody, CdSeS QDs, and target NoV. Notably, this immunosensor emitted fluorescence when excited with UV light, and 0.48 pg mL^{-1} of NoV can be detected (Fig. 6b) [100]. The liposomes encapsulated calcein fluorophore and APTES-functionalized MNPs have been conjugated with the specific antibody. Then, it was attached to target NoV to produce a sandwich-like biosensor (calcein fluorophore/NoV/APTES-MNPs) for NoV detection. This biosensor released fluorescence after the Triton X treatment due to the rupture of the calcein encapsulated liposomes. Using this method, the LOD was as low as 136 copies mL^{-1} [102]. The specific interaction between the antibody and antigen can significantly reduce the background signal, resulting in a higher detection sensitivity. However, this method has a disadvantage due to the usage of less stable liposomes and antibodies.

2.2.4. SARS-CoV-2

The world is currently challenging an unpleasant situation due to the SARS-CoV-2, producing an infectious disease in humans. Indeed, this virus is environmentally stable and transmitted through direct contact and aerosol. To control SARS-CoV-2, an urgent need exists for simple, rapid, and highly sensitive detection methods [103].

2.2.4.1. Colorimetry strategy. The spherical nucleic acids (SNAs) is a thick shell with highly oriented nucleic acids that were conjugated with AuNPs. Moreover, the PCR-amplified SARS-CoV-2 was incubated with AuNP-functionalized SNAs that sustained red color, even after adding the NaCl solution due to the restriction of single component assembly [104]. The thiol functionalized antisense oligonucleotides (ASOs)

capped with AuNPs have a specific interaction with the N-gene of SARS-CoV-2 [105]. Hence, ASO-capped AuNPs sensor was fabricated, which were agglomerated in the presence of the target SARS-CoV-2 N-gene. The RNaseH was introduced to the blue-colored analyte mixture for further signal amplification, producing a precipitate that was visually perceived by the naked eye. This technique enables SARS-CoV-2 detection as low as 0.18 ng μL^{-1} within 10 min [106]. Significantly, the efficacy of the ASO-capped AuNP biosensor was compared with the FDA-approved diagnostic kit for SARS-CoV-2 detection, confirming a good alternative for the commercially available kits. Due to the rapid mutation of SARS-CoV-2, several diagnostic methods fail to sustain its reliability. But, the ASO-capped AuNP biosensor overcomes this limitation by simultaneously detecting the N-gene of SARS-CoV at various positions in the gene sequences.

The clustered regularly interspaced short palindromic repeats (CRISPR) associated nuclease (Cas) (CRISPR/Cas) technique offers to cut the DNA or RNA using the gene-editing technique [107]. Moreover, this method is applied for nucleic acid detection through the colorimetric pathway [108]. Hence, the combination of CRISPR/Cas12a with RT-RPA has been utilized for SARS-CoV-2 detection. In this process, AuNPs were modified with ssDNA, specifically targeting the ORF1ab and N-gene of SARS-CoV-2. After the RT-RPA, Cas12a was activated in the amplified dsDNA. Due to initiating *trans*-cleavage, the capped DNA in the AuNPs' surface was gradually hydrolyzed, triggering the aggregation, and the color of the solution turned blue. Because of RT-RPA and Cas12a, this method can detect even one copy of viral RNA [28].

2.2.4.2. Fluorescence strategy. Recently, HRP-labeled anti-human IgA contained with an H_2O_2/luminol-based biosensor was used for SARS-CoV-2 detection through a chemiluminescence platform [109]. Considering the cost and stability of HRP, a Co–Fe@hemin was synthesized and acted as a nanozyme for detecting the target virus. Indeed, the Co–Fe@hemin nanozyme enhanced the luminol intensity in the presence of SARS-CoV-2 [110]. Using this method, the LOD of SARS-CoV-2 was 0.1 ng mL^{-1}, revealing lower sensitivity than the SPR-based method [106].

3. Electrochemical biosensors for airborne pathogen detection

In an electrochemical biosensor, the interaction between immobilized molecules and target analytes (airborne pathogens) produces electrical signals in the system. Based on the detection principle and application, the produced electrical signal can be read using various techniques such as voltammetry (CV, SWV, DPV), amperometry, and EIS [34–38]. Electrochemical biosensors offer various advantages such as sensitivity, portability, easiness, and rapidity for finding airborne bacteria, and this section briefly addresses them. Tables 4 and 5 summarize a detailed comparison study based on electrochemical biosensors for airborne bacteria and virus detection.

3.1. Airborne bacteria detection

3.1.1. Bacillus anthracis (B. anthracis)

B. anthracis spores have been mostly detected through its biomarker (DPA) in optical biosensors [43,48]. However, this infectious bacterium is directly detected using electrochemical biosensors [111]. Waller et al. established an amperometric immunoassay for detecting *B. anthracis* spores. In this immunoassay, the GOx generated H_2O_2 while oxidizing glucose. The produced H_2O_2 develops an electrical signal when oxidizing ABTS using HRB. Notably, this signal was monitored using an amperometric portable instrument and the detection range was 5×10^3 to 5×10^6 CFU mL^{-1} [112]. More importantly, even minimal signal differences produced in the presence of environmental interferents including soil and altered pH conditions can be detected, exhibiting the strength of the amperometry method. This technique is cost-effective and rapid, and the sensitivity is either superior or comparable to that of the ELISA and LFDs, thus making it a promising tool for detecting *B. anthracis* spores on a portable platform.

As with detecting PA using a colorimetric strategy [23], the SWV technique was performed to detect PA at the picogram level. In this process, the immunoassay was fabricated using Nafion-MWCNTs–bismuth NC film modified glassy carbon electrode (GCE) (BiNPs/Nafion-MWCNTs/GCE) and titanium phosphate NP–cadmium ion-contained anti-PA antibodies (TiP–Cd@PA antibodies). Under optimum conditions, the currents increased when increasing the PA concentration, and LOD was measured as 50 pg mL^{-1} [114]. Typically, the two types of S-layer proteins, such as extractable antigen and surface array protein (Sap), were secreted by *B. anthracis* in the culture medium. Thus, Sap act as a biomarker, and the fabricated bionanolabel (Au–Pd NPs@BNNSs/Ab_2) converted the 4-AP to 4-quinine imine, resulting in

Table 4
A detailed comparison of the electrochemical biosensor for airborne bacteria detection.

Target bacteria	Detection method	Conjugate materials	Linear range	LOD	Time (min)	Real sample	Ref
B. anthracis	Amperometry	ABTS/HRP	10^3–10^6 cfu mL^{-1}	10^2 CFU mL^{-1}	60	–	112
	EIS	aptamer	–	10^3 CFU mL^{-1}	–	Water	113
	SWV	BiNPs/Nafion-MWCNT	0.1–100 ng mL^{-1}	50 pg mL^{-1}	35	Human serum	114
		Ferrocene/dATP	–	0.8 fM	–	Plasmid pXO1	115
	CV	Au/Pd NP/BNNSs	5 pg–100 ng mL^{-1}	1 pg mL^{-1}	3	BSA	116
MTB	CV	AuNTsA	0.01–100 ng μL^{-1}	0.5 ng μL^{-1}	5	–	117
		Oligomer	1 fM–100 pM	0.2 fM	45	–	119
		AuNPs/C60/PAn	0.02–100 pg mL^{-1}	20 fg mL^{-1}	60	Human serum	122
		NH_2–GO/QD	–	8.948×10^{-13}M	50	–	118
	DPV	HANPs/PPy/MWCNT	0.25–200 nM	0.141 nM	–	Sputum	120
		C60NP/N–CNT/GO	1 fg–1 ng mL^{-1}	0.33 fg mL^{-1}	60	Human serum	123
		AuNP@C60/N–GO	10 fM–10 nM	3 fM	60	–	124
		AuNC	0.1–1 $\times 10^5$ fM	0.031 fM	60	BSA	126
		Fe_3O_4@Ag/GQD	0–500 μg mL^{-1}	0.33 ng mL^{-1}	–	BSA	130
		Si NP/CdSe/ZnS QD	40–100 ng mL^{-1}	1.5×10^{-10} g mL^{-1}	–	BSA	131
S. aureus	DPV	ZrO_2/GO	–	3.23×10^{-14} mol L^{-1}	10	–	132
		SWCNT	10–10^7 CFU mL^{-1}	13 CFU mL^{-1}	30	Milk	134
		BC/MWCNT/PEI	10–10^7 CFU mL^{-1}	3 CFU mL^{-1}	30	Milk	138
		aptamer	60–6 $\times 10^7$ CFU mL^{-1}	9 CFU mL^{-1}	–	Water	139
		aptamer	10–10^8 CFU mL^{-1}	8 CFU mL^{-1}	60	Lake water	140
	CV	zeolite/GO	0.5–100 μM	0.1 nM	–	Fruit juice	133
	EIS	AuNR/PDDA/PSS	10^3–10^7 CFU mL^{-1}	2.4×10^2 CFU mL^{-1}	50	Milk	136
S. pneumoniae	CV	oligomer	–	0.5 fM	60	Whole blood	141
	DPV	polyaminophenol	0–200 ng mL^{-1}	54 ng mL^{-1}	–	BSA	143
	SWV	oligomer	0–8 ng mL^{-1}	0.218 ng mL^{-1}	–	BSA	144

Table 5
A detailed comparison of the electrochemical biosensor for airborne virus detection.

Target virus	Detection method	Conjugate materials	Linear range	LOD	Time (min)	Real sample	Ref
Influenza A (H1N1 subtype)	EIS	aptamer	–	0.9 pg μL^{-1}	30	BSA	17
		BDD	–	1 fg μL^{-1}	–	BSA	147
		TrGO	–	33 PFU mL^{-1}		Saliva	148
	DPV	Cys/oligomer	–	0.002 ng μL^{-1}	30	–	149
		AuNP−MNP−CNT	1 μg–100 fg mL^{-1}	13.66 fg mL^{-1}	–	BSA	150
	Amperometry	antibody	1–10^4 PFU mL^{-1}	0.5 PFU mL^{-1}	–	–	151
Avian influenza A (H5N1 subtype)	EIS	aptamer	–	0.0128 HAU	30	–	154
		AuNP/aptamer	16–0.125 HAU	0.25 HAU	45	–	155
	CV	pAuNP	–	1 pM	–	Chicken serum	156
	Amperometry	ZnO NR	–	1 pg mL^{-1}	–	BSA	157
Norovirus	EIS	Cys/Nor-1 peptide	–	1.44 μg mL^{-1}	–	Fetal bovine serum (FBS)	158
		Specific binding peptides	0–10^5 copies mL^{-1}	1.7 copies mL^{-1}	30	FBS	159
		WS_2NF/AuNP	0–10^4 copies mL^{-1}	2.3 copies mL^{-1}	60	FBS	161
	CV	ConA/ALP	10^2–10^4 copies mL^{-1}	35 copies mL^{-1}	60	–	162
	Potentiometer	AuNP/MNP/graphene	0.01 pg–1 ng mL^{-1}	1.16 pg mL^{-1}	–	BSA	163
	DPV	AuNP/graphene	100 pM–3.5 nM	100 pM	30	–	36
SARS-CoV-2	Amperometry	Co/TiO_2 NT	14–1400 nM	0.7 nM	–	–	167
	EIS	antibody	–	20 μg mL^{-1}	45	BSA	168
	DPV	Au@Pt/MIL–53(Al)	0.025–50 ng mL^{-1}	8.33 pg mL^{-1}	60	Human serum	169
		sulfocalix[8]arene/GO	–	200 copies mL^{-1}	–	Saliva	170
		RPA amplicon/thiol-modified primers	–	3.925 fg μL^{-1}	20	–	171

redox peaks that were monitored by CV. Significantly, this proposed immunosensor exhibited a good linear range from 5 pg mL^{-1} to 100 ng mL^{-1}, and the LOD of *B. anthracis* Sap was 1 pg mL^{-1} (Fig. 7a) [116]. Interestingly, the biomarker Sap is only secreted by *B. anthracis* and other species of *Bacillus* will not produce it. Therefore, this method has high selectivity toward *B. anthracis* detection compared with other techniques. Substantially, the fabricated Au–Pd NPs@BNNSs/Ab_2 immunosensor can quantify the Sap within 1 h due to its high catalytic activity, showing the importance of this electrochemical biosensor.

3.1.2. *Mycobacterium tuberculosis (MTB)*

The Au nanotubes array (AuNTsA) has a higher electron transfer capacity than the bare Au electrode due to its high surface area; thus, AuNTsA was synthesized using the electrochemical deposition method. To construct the biosensor, the probe DNA was immobilized on the AuNTsA surface, and complementary DNA was hybridized on it. In the process, the electron transfer of redox indicator $[Fe(CN)_6]^{3-/4-}$ was monitored using CV. The target DNA concentration from 0.01 ng μL^{-1} to 100 ng μL^{-1} exhibited a good linear range [117]. In general, the AuNTsA is more delicate and easily damaged. However, this method simply modified the electrodeposition method and produced stable AuNTsA. Moreover, the produced AuNTsA are well separated from each other, which acted as individual electrodes resulting in a substantial improvement in the detection process. Significantly, the AuNTsA electrode is more beneficial compared with the bare Au electrode due to the radial diffusion of ions in constructing efficient electrochemical biosensors. In addition, the fabricated electrode sustained its efficacy toward MTB detection up to three weeks, confirming the stability of the AuNTsA-based electrochemical biosensor [117].

Sypabekova et al. established an aptamer-based technique for MPT64 protein detection, which is an immunogenic polypeptide of MTB. Typically, the aptamer corresponding to the MPT64 protein was designed using the SELEX technique. The designed aptamer was attached to the electrode surface using the thiolated linker. The current fluctuations occurred when introducing the MPT64 protein on the biosensor, monitored using EIS [121]. The fullerene (C60)-incorporated NCs were exclusively involved in MPT64 protein detection due to their electron transfer capacity [122,123]. The MPT64 aptamer was immobilized on the AuNPs@C-60/N-CNT/GO NC surface, developing a sandwich biosensor using polyethyleneimine (PEI)-functionalized MOF. The tetraoctylammonium bromide (TOAB) was used to enhance the redox activity of this sandwich biosensor in the presence of the MPT64 protein (Fig. 7b) [123]. Using this method, the LOD was measured as low as 0.33 fg mL^{-1}, revealing higher sensitivity than the SPR-based method [60].

The IS6110 gene is found at various sites in the MTB genome. Thus, this gene sequence detection was helpful for MTB diagnosis, and the DPV-based electrochemical technique was widely used to monitor the IS6110 gene [124–127]. Arginine contained an active amino group ($-NH_2$), providing an excellent platform for hybridization between the probe DNA and target DNA. Using MB as the redox signal developer in the DPV technique, up to 4.4 nM of the IS6110 gene was detected [125]. However, the proposed method has lower performance than the target DNA-induced recycling amplification and enzyme-assisted signal amplification-based strategies [126,127]. The culture-filtered protein (CFP-10) is also used as a biomarker to diagnose TB at an earlier stage [128–131]. Tufa et al. devised an immunosensor based on the antigen-antibody interaction. Initially, the CFP-10 antigen was binding with Fe_3O_4@Ag/GQD NCs. The CFP-10 antibody was conjugated with AuNPs which were employed for signal amplification. In this process, the electron transfer and binding ability increased due to the large surface area of the NCs. Thus, the resultant immunosensor revealed high specificity and reasonable LOD against the CFP10 antigen [130]. Significantly, Fe_3O_4 NPs in the nanotriplex (Fe_3O_4@Ag/GQD) sensor enabled facile transportation of reactant and product at the electrode surface. Moreover, AgNPs and GQDs enhanced the electrical conductivity and captured more CFP-10 antigen due to their high surface area. Hence, the nanotriplex (Fe_3O_4@Ag/GQD) sensor achieved good electrochemical performance toward MTB detection, and the properties of these nanomaterials make them a promising candidate to fabricate an efficient electrochemical biosensor for the detection of other pathogenic bacteria in the future.

3.1.3. *Staphylococcus aureus (S. aureus)*

S. aureus bacteria causes severe health-related issues; thus, electrochemical biosensors were employed for its detection [16,33]. Sun et al. established a novel electrode surface containing ZrO_2/GO for hybridization between the probe ssDNA and target ssDNA. The MB easily

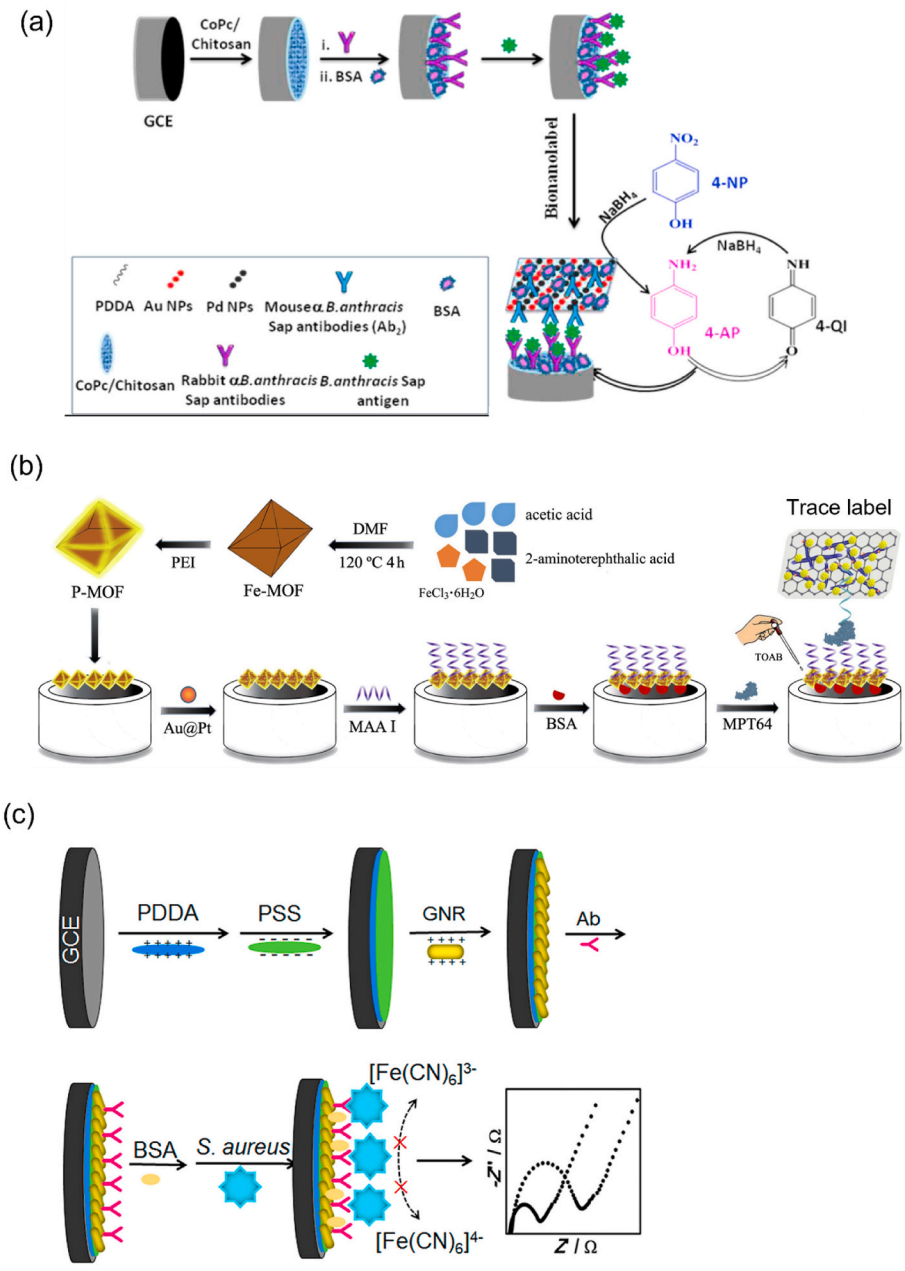

Fig. 7. (a) Proposed electrochemical immunosensor for the detection of *B. anthracis* Sap based on the generation of the redox peaks upon the conversion of the 4-AP to 4-quinine imine. Reproduced from the published article [116]. (b) Target MPT64 sandwiched between the PEI@MOF-modified electrode and the tracer label. TOBA developed the electrical signal in the presence of target bacteria. Reproduced from the published article [123]. (c) Schematic showing a label-free electrochemical immunosensor using PDDA, PSS, and AuNR on the GCE for *S. aureus* detection. Reproduced from the published article [136].

attaches to dsDNA and functions as a redox indicator in the electrochemical process. Thus, the *S. aureus*-contained electrode was dipped in the MB solution and monitored the redox signal variation using the DPV technique. Notably, this fabricated biosensor detected the *S. aureus* as low as 3.23×10^{-14} mol L^{-1} [132]. Electrochemical immunosensors were impeccably applied to *S. aureus* detection [134–137]. AuNRs have good electron conductivity and were functionalized with poly(diallyldimethylammonium chloride) (PDDA) and polystyrene sulfonate (PSS) on the GCE surface for binding the antibodies. The immobilized specific antibodies competently captured the *S. aureus* cell, and electron transfer on the GCE surface was blocked. Significantly, EIS was used to measure the variation of electron transfer resistance of $Fe(CN)_6^{3-/4-}$ (Fig. 7c). The proposed immunosensor could detect the bacteria as low as 2.4×10^2 CFU mL^{-1} [136]. In this technique, the simplest self-assembled process was utilized which can control biomolecule density and orientation at a solid-liquid interface resulting in a highly sensitive detection. Most of the *S. aureus* cells were efficiently captured on the PDDA/PSS/AuNRs/Ab surface without nonspecific adsorption revealing the advantages of the self-assembled immunosensor. Using this method, the whole *S. aureus* cell has been detected, which eliminated the complex sample preparation processes [136].

In terms of cost and stability of antibodies, devising immunosensors have received increasing challenges recently. Hence, a novel material, such as bacterial cellulose (BC), was modified with MWCNTs for *S. aureus* detection. The BC/MWCNTs nanohybrid was further treated with PEI to obtain a positive charge on the surface. Finally, the bacterial phage was immobilized on the BC/MWCNT/PEI surface based on the electrostatic interaction. The phage concentration determined the current responses in the biosensor, and up to 3 CFU mL^{-1} of *S. aureus* was detected using the DPV method [138]. Significantly, this method was first reported to differentiate live *S. aureus* cells from the mixture of live/dead cells based on the utilization of the bacteriophages and BC. The BC/MWCNT/PEI film has high lytic activity and thus phages were actively immobilized on its surface, providing excellent sensitivity and selectivity toward live *S. aureus* cells detection. Moreover, the immobilized phages could be in a humid environment due to the never-dried

nature of BC, resulting in bacteriophages with BC-contained electrochemical biosensors that are highly stable and portable.

3.1.4. *Streptococcus pneumoniae (S. pneumoniae)*

Electrochemical biosensors can detect *S. pneumoniae* rapidly [141]. Typically, electrode surface modification with polymer components has shown enormous benefits in the electrochemical biosensor field [138, 142]. Ferreira et al. modified the graphite electrode surface based on electropolymerization using 4-AP. Due to polymerization, the surface contained –NH_2 and –OH groups, which easily attract oligonucleotides and hybridized with the target ssDNA, producing dsDNA on the electrode surface. Ethidium bromide (EB) functions as an indicator that was efficiently intercalated into the dsDNA. Notably, the current responses generated by EB in the presence of *S. pneumoniae* were monitored using

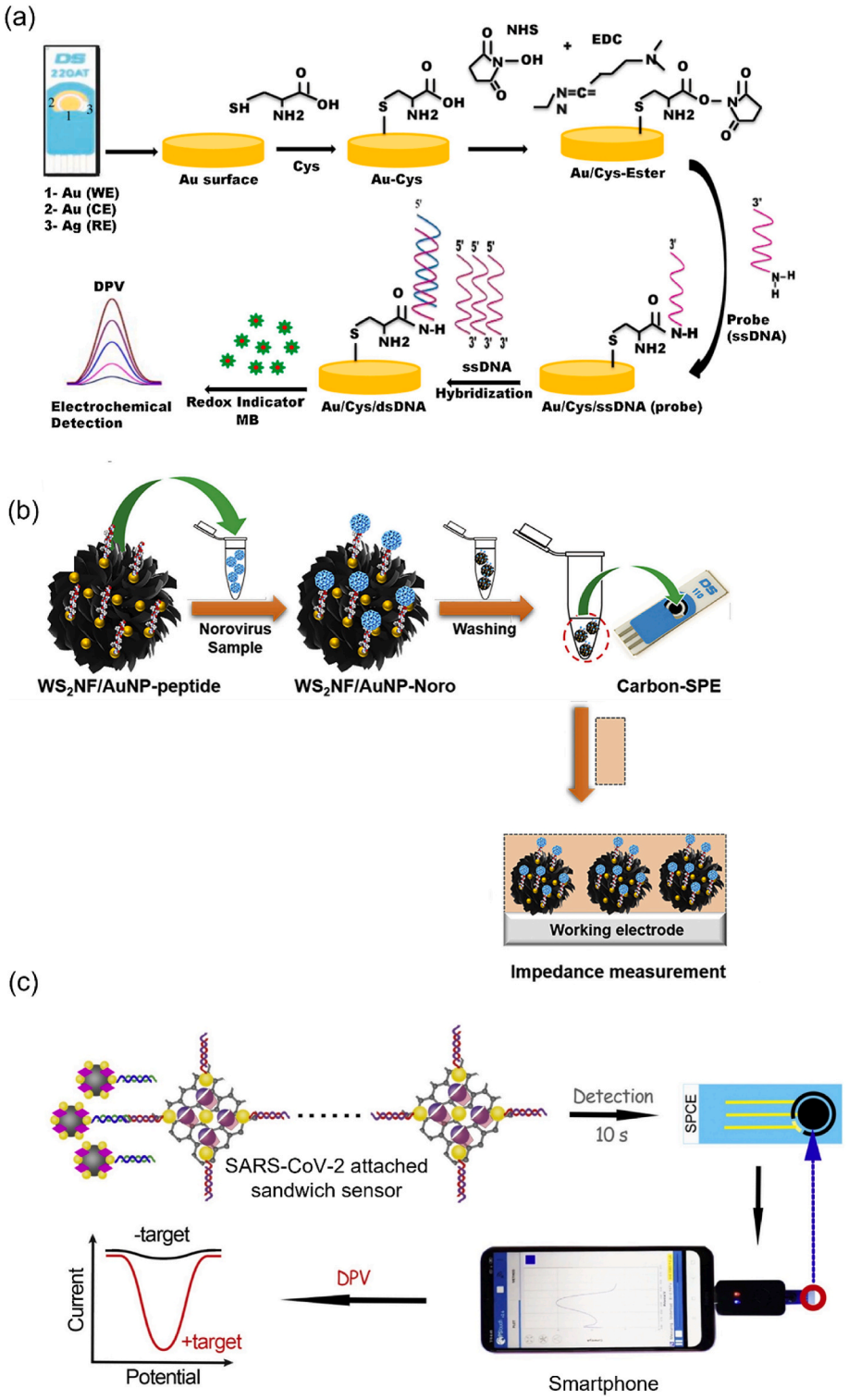

Fig. 8. (a) Schematic fabrication of electrochemical biosensor using Cys-linked probe for H1N1 detection. Reproduced from the published article [149]. (b) Schematic representation for Norovirus detection using a WS_2NF/AuNP-peptide electrochemical biosensor. Reproduced from the published article [161]. (c) Process of super sandwich biosensor for the detection of SARS-CoV-2 using a smartphone. Reproduced from the published article [170].

DPV analysis [143]. Using this process, the LOD was 54 ng mL^{-1}, revealing lower sensitivity than the colorimetric LAMP-based method [8].

3.2. Airborne virus detection

3.2.1. Influenza A (H1N1 and H3N2)

Each year, influenza A affects two billion people, according to the WHO report. Early detection is critical to control the disease, and electrochemical biosensors are increasingly used in identifying these viruses [145]. Matsubara et al. focused on the sialic acid-mimic peptide immobilized on a boron-doped diamond (BDD) electrode using click chemistry for detecting infectious viruses. Significantly, the H1N1 and H3N2 were identified in the limit of 20–500 PFU using EIS analysis [146]. Ravina et al. established a Cys-coated Au-SPE for immobilizing the probe ssDNA. Then, it was hybridized with target ssDNA to produce dsDNA on the electrode surface. Using DPV analysis, 0.002 ng μL^{-1} of H1N1 was detected (Fig. 8a) [149]. This study utilized an SPE due to its advantages such as high electrical conductivity, biocompatibility, and stability in various temperatures and pH compared with the other electrodes. Moreover, Cys was easily adsorbed on the SPE surface due to the presence of Au which provided a site to capture the probe DNA on the electrode surface for the electrochemical detection of H1N1. Significantly, this study followed a simple methodology and thus could be employed as a POC diagnosis tool for influenza virus detection.

3.2.2. Avian influenza A (AIV)

The H5N1 AIV can rapidly mutate and combine with other subtypes to become a more dangerous pathogen. To prevent its transmission rate, earlier diagnosis is much better, and electrochemical biosensors contributed significantly to this purpose [152]. Lin et al. implemented an impedance immunosensor for H5N1 detection in a real sample. Wet etching microfabrication was employed to modify the electrode and functionalized it with H5N1 antibodies. The impedance magnitude increased when the electrode captured H5N1, and the LOD of this method was 0.2 HAU 50 μL^{-1} [153]. Compared with the dry-etching process, the improved wet-etching process was utilized in this study which competently reduced the production cost of the interdigitated microelectrode. Moreover, the fabricated electrode can be used at least five times after cleaning with NaOH and HCl solution, however, the recycling process of the electrode may be challenging in the real sample analysis. Significantly, this immunosensor was tested on the chicken swab to identify the H5N1, producing almost comparable accuracy with the RT- PCR method [153]. Indeed, ZnO NR has a high isoelectric point (IEP), stimulating the electrostatic interaction with the lower IEP of AIV antibodies. Using this concept, Han et al. developed a microfluidic electrochemical immunosensor for H5N1 detection [157]. Amperometry analysis measured the oxidation current produced in the process, and LOD was 1 pg mL^{-1}, showing equal sensitivity with the SPR-based method [88].

3.2.3. Norovirus (NoV)

NoV is a lethal human pathogen effectively monitored by electrochemical biosensors due to simplified sample preparation and high sensitivity [6]. Hwang et al. adopted a peptide (Nor-1 peptide)-based evolutionary phage display technique to monitor NoV [158]. In the process, Cys was incorporated into the Nor-1 peptide and immobilized to an Au electrode to produce a biosensor (Au/Cys/Nor-1 peptide). When recombinant noroviral capsid proteins (rP2) were actively attached to the Au/Cys/Nor-1 peptide, a significant increase in impedance was observed due to electrode surface blocking. Using this method, LOD was measured as 1.44 μg mL^{-1}, showing lower performance than the fluorescence-based biosensor [100]. The hydrothermally synthesized 2D-tungsten disulfide (WS_2) nanoflowers (NF) have unique electronic properties. Introducing metal NPs enhanced their charge carrier mobility and thermal conductivity [160]. Hence, Baek et al. synthesized AuNP-decorated WS_2NF and combined it with the bioreceptor attached Cys for capturing the target NoV. Based on EIS analysis, the LOD for NoV was 2.37 copies mL^{-1} (Fig. 8b) [161]. ConA specifically targeted NoV, not capturing other viruses, such as hepatitis A and hepatitis E. Thus, ConA was attached to a nanostructured Au electrode and immobilized with ALP-contained secondary antibodies. Notably, 4-aminophenyl phosphate was changed to 4-AP due to the presence of ALP in the electrode, and a redox signal was generated when 4-AP was oxidized to 4-quinone imine. CV revealed that the oxidation current increased while increasing the NoV concentration [162]. The detection limit was 35 copies mL^{-1}, disclosing higher efficiency than the fluorescence-based method [102].

3.2.4. SARS-CoV-2

Optical biosensors considerably contributed to SARS-CoV-2 detection, which further demands various analytical techniques due to the high transmittance rate of this infectious virus [164,166]. Hence, electrochemical biosensors were developed with high sensitivity toward SARS-CoV-2 [165]. The receptor-binding domain (RBD) of spike protein is present on the SARS-CoV-2 surface, which can be detected using cobalt-functionalized TiO_2 nanotubes. Amperometry analysis detected the RBD protein in the range of 14–1400 nM within 30 s; thus, this sensor could be used in the rapid diagnostic process [167]. Calixarene is an example of macrocyclic molecules exhibiting excellent enrichment capability to electrochemical indicators, such as MB and toluidine blue (TB). Hence, Zhao et al. fabricated a super sandwich-type electrochemical biosensor based on GO functionalized with p-sulfocalix [8] arene to enrich TB for detecting SARS-CoV-2. Significantly, the GO functionalized p-sulfocalix [8] arene electrochemical biosensor has higher sensitivity (85.5%) than the RT-qPCR (56.5%) when tested with 35 SARS-CoV-2 positive samples. Notably, this super sandwich-type technology does not demand amplification and reverse transcription processes for the detection of SARS-CoV-2. More importantly, this electrochemical biosensor has first established the detection of SARS-CoV-2 based on the smartphone platform (Fig. 8c) [170].

4. Conclusions

Considering the severity and high transmission rate of airborne pathogens, accurate and rapid detection methods are critical. Traditional methods are either expensive and time-consuming or have low sensitivity toward detecting contagious pathogens. Hence, this review focused on emerging techniques, such as optical and electrochemical biosensors to find airborne pathogens, even at low concentrations. Optical biosensors have been inspired by three strategies, such as SPR, colorimetry, and fluorescence used for pathogen detection. Metal NPs, including AuNPs and AgNPs, have unique SPR properties that help to find airborne bacteria and viruses in a short time. In the colorimetry process, a label-free assay is a direct method, that is, the transducer surface generates a distinguishable color in the presence of target analytes due to the biochemical reaction. Significantly, the labeled assay developed an intense color when the target analytes were sandwiched between the capture and fluorophores labeled detector agents. These optical biosensors are easy to fabricate, show prompt results, and have high sensitivity to airborne pathogen detection. Another approachable electrochemical process was unprecedently employed in airborne pathogen detection due to its precision, rapidity, and sensitivity. Moreover, the generated electrical signal based on the interaction between the fabricated electrode and target analytes can easily be measured through various strategies, such as DPV, CV, SWV, amperometry, and EIS. Although there is enormous benefit from the optical and electrochemical biosensors, some critical aspects must be considered to convert them into on-site applications.

5. Challenges and future perspectives

(i). Devising immunosensors in optical/electrochemical techniques typically used antibodies, antigens, and enzymes (HRP) for producing higher sensitivity toward airborne pathogen detection. However, the stabilities of these biological substances are low, having a shorter shelf life and extra care must be taken to sustain their stability. Hence, immunosensors could not be applied in resource-poor settings.

(ii). Aptamers provide excellent benefits over antibodies in terms of stability, production cost, and synthesis. Hence, it plays a significant role to develop aptasensors for airborne pathogen detection, where they can function as biorecognition components. However, the shorter-length aptamers do not have high affinities with biomolecules, and longer sequences lead to aggregation or misfolding, affecting the yield of chemical synthesis. Therefore, the perfect length of aptamers must be optimized before fabricating the aptasensor. Furthermore, the immobilization of aptamers is complicated because it relies on adding biotin/streptavidin or a chemical reaction (EDC/NHS coupling), making it an expensive process.

(iii). Nanozymes have high stability and can be used for pathogen identification based on peroxidase-like activities. However, its synthetic methods are too intricate and offer less reproducibility. Therefore, the advancement of easy-to-prepare methods and fabrication of nanozyme-based highly sensitive biosensors for airborne pathogen detection are needed.

(iv). The inorganic material containing fluorescence probes (optical biosensor) has higher stability and improved sensitivity against infectious pathogens. Furthermore, the ratiometric fluorescence probes measured the variation of the fluorescence intensity ratio developed in the presence of the pathogen and obtained an accurate result. However, each fluorophore has individual fluorescence intensities and many experiments must be conducted using a combination of different fluorophores to obtain perfect ratiometric fluorescence sensors. Therefore, the fluorescence technique is considered expensive and laborious.

(v). Due to technology improvements, the nucleic acid amplification-based method is widely used for airborne pathogen detection, offering improved sensitivity and fast responses over other techniques. However, this method requires expensive reagents, sophisticated equipment, and a modernized laboratory to perform the biochemical reaction. To simplify this technique, the device should be modified as a portable platform to identify the pathogen competently.

(vi). PDA-fabricated biosensors have received much attention due to their characteristic chromatic properties and are employed in colorimetric infectious disease monitoring, but only limited experiments have been performed so far. Thus, elaborate research based on PDA biosensors is necessary to apply for on-site applications.

(vii). In the electrochemical biosensor, various electrodes are available, and choosing a suitable electrode for devising the potential sensor is critical. Furthermore, recently developed electrochemical biosensors have many advantages in terms of miniaturization and portability. Nevertheless, the device fabrication process is time-consuming and costly, which is a demerit and should be considered before designing effective electrochemical biosensors.

(viii). Colorimetric biosensors using the LFIA technique produced a successful kit that is commercially available for HIV and pregnancy tests. Similarly, airborne bacteria (*B. anthracis*, MTB, and *S. pneumoniae*) were monitored using the LFIA-based colorimetric biosensor and other infectious pathogens have to be detected using a similar platform due to its uniqueness. Despite the LFIA being a qualitative assay, they are desirable for using POCT due to their simplicity, portability, and ease to see the obtained result with the naked eye. Overall, each technique has its advantages and limitations, but further research is needed for each technique to become an attractive POCT diagnostic kit. Finally, this review provided an in-depth knowledge of optical and electrochemical biosensors based on consolidated recently published articles; thus, it will benefit those working in the field of airborne pathogen detection.

Declaration of competing interest

The authors declare that they have no known competing financial interests or personal relationships that could have appeared to influence the work reported in this paper.

Data availability

No data was used for the research described in the article.

Acknowledgments

This work was supported by the National Research Foundation of Korea (NRF) grant funded by the Korea government (MSIT) (No. NRF 2020R1A2B5B01001971) and also by Basic Science Research Program through the National Research Foundation of Korea (NRF) funded by the Ministry of Education (2021R1A6A1A03038996).

Abbreviations

WHO	World Health Organization
POCT	Point of Care Test
PCR	Polymerase Chain Reaction
LAMP	Loop-mediated isothermal amplification
RCA	Rolling Circle Amplification
RPA	Recombinase Polymerase Amplification
ELISA	Enzyme-Linked Immunosorbent Assay
SPR	Surface Plasmon Resonance
NPs	Nanoparticles
MOFs	Metal-Organic Frameworks
MNPs	Magnetic Nanoparticles
CNTs	Carbon Nanotubes
CV	Cyclic Voltammetry
SWV	Square-Wave Voltammetry
DPV	Differential Pulse Voltammetry
EIS	Electrochemical Impedance Spectroscopy
B. anthracis	*Bacillus anthracis*
MTB	*Mycobacterium tuberculosis*
S. aureus	*Staphylococcus aureus*
S. pneumoniae	*Streptococcus pneumoniae*
DPA	Dipicolinic acid
LOD	Limit of Detection
EBT	Eriochrome Black T
UCNPs	Upconversion Nanoparticles
PA_{83}	Anthrax Protective Antigen
TMB	3,3′,5,5′–tetramethylbenzidine
H_2O_2	Hydrogen peroxide
LFIA	Lateral-Flow Immunochromatographic Assay
HRP	Horseradish Peroxidase
CDs	Carbon Dots
Ag85B	MTB antigen 85B
MNase	Micrococcal Nuclease
ALP	Alkaline Phosphatase
NCs	Nanocomposites
ConA	Concanavalin A
AIV	Avian Influenza A
4-AP	4-aminophenol

NoV	Norovirus
LF	Lactoferrin
6-FAM	6-carboxyfluorescein
SNAs	Spherical Nucleic Acids
ASOs	Antisense Oligonucleotides
SPE	Screen-Printed Electrode
Sap	Surface array protein
MB	Methylene Blue
C60	Fullerene
TOAB	Tetraoctylammonium bromide
SWCNTs	Single-Walled Carbon Nanotubes
GCE	Glassy Carbon Electrode
PDDA	Poly(diallyldimethylammonium chloride)
PSS	Polystyrene sulfonate
BC	Bacterial Cellulose
EB	Ethidium Bromide
CFP10	Culture-filtered protein
PspA	Pneumococcal surface protein A
BDD	Boron-Doped Diamond
Cys	Cysteine
RBD	Receptor-Binding Domain

References

[1] B. Acharya, A. Acharya, S. Gautam, S.P. Ghimire, G. Mishra, N. Parajuli, B. Sapkota, Advances in diagnosis of Tuberculosis: an update into molecular diagnosis of Mycobacterium tuberculosis, Mol. Biol. Rep. 47 (2020) 4065–4075.

[2] S.M. Kim, J. Kim, S. Noh, H. Sohn, T. Lee, Recent development of aptasensor for influenza virus detection, Biochip J 14 (2020) 1–13.

[3] J.I. Lee, S.C. Jang, J. Chung, W.K. Choi, C. Hong, G.R. Ahn, S.H. Kim, B.Y. Lee, W. J. Chung, Colorimetric allergenic fungal spore detection using peptide-modified gold nanoparticles, Sensor. Actuator. B Chem. 327 (2021), 128894.

[4] J. Ma, M. Du, C. Wang, X. Xie, H. Wang, Q. Zhang, Advances in airborne microorganisms detection using biosensors: a critical review, Front. Environ. Sci. Eng. 15 (2021) 1–19.

[5] Y. Choi, J.H. Hwang, S.Y. Lee, Recent trends in nanomaterials-based colorimetric detection of pathogenic bacteria and viruses, Small Methods 2 (2018), 1700351.

[6] S.K. Bhardwaj, N. Bhardwaj, V. Kumar, D. Bhatt, A. Azzouz, J. Bhaumik, K. H. Kim, A. Deep, Recent progress in nanomaterial-based sensing of airborne viral and bacterial pathogens, Environ. Int. 146 (2021), 106183.

[7] R. Sivakumar, V.P. Dinh, N.Y. Lee, Ultraviolet-induced in situ gold nanoparticles for point-of-care testing of infectious diseases in loop-mediated isothermal amplification, Lab Chip 21 (2021) 700–709.

[8] H. Wang, Z. Ma, J. Qin, Z. Shen, Q. Liu, X. Chen, H. Wang, Z. An, W. Liu, M. Li, A versatile loop-mediated isothermal amplification microchip platform for Streptococcus pneumoniae and Mycoplasma pneumoniae testing at the point of care, Biosens. Bioelectron. 126 (2019) 373–380.

[9] R.W. Chan, M.C. Chan, J.M. Nicholls, J.M. Peiris, Use of ex vivo and in vitro cultures of the human respiratory tract to study the tropism and host responses of highly pathogenic avian influenza A (H5N1) and other influenza viruses, Virus Res. 178 (2013) 133–145.

[10] M.L. Sin, K.E. Mach, P.K. Wong, J.C. Liao, Advances and challenges in biosensor-based diagnosis of infectious diseases, Expert Rev. Mol. Diagn. 14 (2014) 225–244.

[11] P.J. Tighe, R.R. Ryder, I. Todd, L.C. Fairclough, ELISA in the multiplex era: potentials and pitfalls, Proteonomics Clin. Appl. 9 (2015) 406–422.

[12] K. Dziąbowska, E. Czaczyk, D. Nidzworski, Detection methods of human and animal influenza virus—current trends, Biosensors 8 (2018) 94.

[13] S.V. Vemula, J. Zhao, J. Liu, X. Wang, S. Biswas, I. Hewlett, Current approaches for diagnosis of influenza virus infections in humans, Viruses 8 (2016) 96.

[14] S. Hassanpour, B. Baradaran, M. Hejazi, M. Hasanzadeh, A. Mokhtarzadeh, M. de la Guardia, Recent trends in rapid detection of influenza infections by bio and nanobiosensor, Trends Anal. Chem. 98 (2018) 201–215.

[15] A. Mansour, S. Tammam, A. Althani, H.M. Azzazy, A single tube system for the detection of Mycobacterium tuberculosis DNA using gold nanoparticles based FRET assay, J. Microbiol. Methods 139 (2017) 165–167.

[16] Y. Sun, X. He, J. Ji, M. Jia, Z. Wang, X. Sun, A highly selective and sensitive electrochemical CS–MWCNTs/Au-NPs composite DNA biosensor for Staphylococcus aureus gene sequence detection, Talanta 141 (2015) 300–306.

[17] C. Bai, Z. Lu, H. Jiang, Z. Yang, X. Liu, H. Ding, H. Li, J. Dong, A. Huang, T. Fang, Y. Jiang, Aptamer selection and application in multivalent binding-based electrical impedance detection of inactivated H1N1 virus, Biosens. Bioelectron. 110 (2018) 162–167.

[18] Y. Liu, L. Zhang, W. Wei, H. Zhao, Z. Zhou, Y. Zhang, S. Liu, Colorimetric detection of influenza A virus using antibody-functionalized gold nanoparticles, Analyst 140 (2015) 3989–3995.

[19] S. Wang, W. Deng, L. Yang, Y. Tan, Q. Xie, S. Yao, Copper-based metal–organic framework nanoparticles with peroxidase-like activity for sensitive colorimetric detection of Staphylococcus aureus, ACS Appl. Mater. Interfaces 9 (2017) 24440–24445.

[20] L. Xu, R. Wang, L.C. Kelso, Y. Ying, Y. Li, A target-responsive and size-dependent hydrogel aptasensor embedded with QD fluorescent reporters for rapid detection of avian influenza virus H5N1, Sensor. Actuator. B Chem. 234 (2016) 98–108.

[21] J. Zhou, R. Fu, F. Tian, Y. Yang, B. Jiao, Y. He, Dual enzyme-induced Au–Ag alloy nanorods as colorful chromogenic substrates for sensitive detection of Staphylococcus aureus, ACS Appl. Bio Mater. 3 (2020) 6103–6109.

[22] X. Zhang, D. Wu, X. Zhou, Y. Yu, J. Liu, N. Hu, H. Wang, G. Li, Y. Wu, Recent progress in the construction of nanozyme-based biosensors and their applications to food safety assay, Trends Anal. Chem. 121 (2019), 115668.

[23] I.N. Larkin, V. Garimella, G. Yamankurt, A.W. Scott, H. Xing, C.A. Mirkin, Dual-readout sandwich immunoassay for device-free and highly sensitive anthrax biomarker detection, Anal. Chem. 92 (2020) 7845–7851.

[24] S. Oh, J. Kim, V.T. Tran, D.K. Lee, S.R. Ahmed, J.C. Hong, J. Lee, E.Y. Park, J. Lee, Magnetic nanozyme-linked immunosorbent assay for ultrasensitive influenza A virus detection, ACS Appl. Mater. Interfaces 10 (2018) 12534–12543.

[25] S.R. Ahmed, J. Kim, T. Suzuki, J. Lee, E.Y. Park, Enhanced catalytic activity of gold nanoparticle-carbon nanotube hybrids for influenza virus detection, Biosens. Bioelectron. 85 (2016) 503–508.

[26] J. Thapa, B. Maharjan, M. Malla, Y. Fukushima, A. Poudel, B.D. Pandey, K. Hyashida, S.V. Gordon, C. Nakajima, Y. Suzuki, Direct detection of Mycobacterium tuberculosis in clinical samples by a dry methyl green loop-mediated isothermal amplification (LAMP) method, Tuberculosis 117 (2019) 1–6.

[27] S.V. Hamidi, H. Ghourchian, Colorimetric monitoring of rolling circle amplification for detection of H5N1 influenza virus using metal indicator, Biosens. Bioelectron. 72 (2015) 121–126.

[28] W.S. Zhang, J. Pan, F. Li, M. Zhu, M. Xu, H. Zhu, Y. Yu, G. Su, Reverse transcription recombinase polymerase amplification coupled with CRISPR-cas12a for facile and highly sensitive colorimetric SARS-CoV-2 detection, Anal. Chem. 93 (2021) 4126–4133.

[29] J. Wang, H. Li, T. Li, L. Ling, Determination of bacterial DNA based on catalytic oxidation of cysteine by G-quadruplex DNAzyme generated from asymmetric PCR: application to the colorimetric detection of Staphylococcus aureus, Microchim. Acta 185 (2018) 1–9.

[30] A.T. Bayraç, S.I. Donmez, Selection of DNA aptamers to Streptococcus pneumonia and fabrication of graphene oxide based fluorescent assay, Anal. Biochem. 556 (2018) 91–98.

[31] O. Pashchenko, T. Shelby, T. Banerjee, S. Santra, A comparison of optical, electrochemical, magnetic, and colorimetric point-of-care biosensors for infectious disease diagnosis, ACS Infect. Dis. 4 (2018) 1162–1178.

[32] J. Huang, Z. Xie, Z. Xie, S. Luo, L. Xie, L. Huang, Q. Fan, Y. Zhang, S. Wang, T. Zeng, Silver nanoparticles coated graphene electrochemical sensor for the ultrasensitive analysis of avian influenza virus H7, Anal. Chim. Acta 913 (2016) 121–127.

[33] K. Bekir, H. Barhoumi, M. Braiek, A. Chrouda, N. Zine, N. Abid, A. Maaref, A. Bakhrouf, H.B. Ouada, N. Jaffrezic-Renault, H.B. Mansour, Electrochemical impedance immunosensor for rapid detection of stressed pathogenic Staphylococcus aureus bacteria, Environ. Sci. Pollut. Res. 22 (2015) 15796–15803.

[34] M. Raveendran, A.F. Andrade, J. Gonzalez-Rodriguez, Selective and sensitive electrochemical DNA biosensor for the detection of Bacillus anthracis, Int. J. Electrochem. Sci. 11 (2016) 763–776.

[35] S. Eissa, H.A. Alhadrami, M. Al-Mozaini, A.M. Hassan, M. Zourob, Voltammetric-based immunosensor for the detection of SARS-CoV-2 nucleocapsid antigen, Microchim. Acta 188 (2021) 1–10.

[36] R. Chand, S. Neethirajan, Microfluidic platform integrated with graphene-gold nano-composite aptasensor for one-step detection of norovirus, Biosens. Bioelectron. 98 (2017) 47–53.

[37] A. Sotillo, M. Pedrero, M. de Pablos, J.L. García, E. García, P. García, J. M. Pingarrón, J. Mingorance, S. Campuzano, Clinical evaluation of a disposable amperometric magneto-genosensor for the detection and identification of Streptococcus pneumoniae, J. Microbiol. Methods 103 (2014) 25–28.

[38] K. Siuzdak, P. Niedziałkowski, M. Sobaszek, T. Łęga, M. Sawczak, E. Czaczyk, K. Dziąbowska, T. Ossowski, D. Nidzworski, R. Bogdanowicz, Biomolecular influenza virus detection based on the electrochemical impedance spectroscopy using the nanocrystalline boron-doped diamond electrodes with covalently bound antibodies, Sensor. Actuator. B Chem. 280 (2019) 263–271.

[39] R. Zhou, Q. Zhao, K.K. Liu, Y.J. Lu, L. Dong, C.X. Shan, Europium-decorated ZnO quantum dots as a fluorescent sensor for the detection of an anthrax biomarker, J. Mater. Chem. C 5 (2017) 1685–1691.

[40] Y. Luo, L. Zhang, L. Zhang, B. Yu, Y. Wang, W. Zhang, Multiporous terbium phosphonate coordination polymer microspheres as fluorescent probes for trace anthrax biomarker detection, ACS Appl. Mater. Interfaces 11 (2019) 15998–16005.

[41] A.A. Zasada, Detection and identification of Bacillus anthracis: from conventional to molecular microbiology methods, Microorganisms 8 (2020) 125.

[42] M. Verma, N. Kaur, N. Singh, Naphthalimide-based DNA-coupled hybrid assembly for sensing Dipicolinic acid: a biomarker for Bacillus anthracis spores, Langmuir 34 (2018) 6591–6600.

[43] S. Yin, C. Tong, Europium (III)-Modified silver nanoparticles as ratiometric colorimetric and fluorescent dual-mode probes for selective detection of dipicolinic acid in bacterial spores and lake waters, ACS Appl. Nano Mater. 4 (2021) 5469–5477.

[44] Z.H. Cheng, X. Liu, S.Q. Zhang, T. Yang, M.L. Chen, J.H. Wang, Placeholder strategy with upconversion Nanoparticles– eriochrome black T conjugate for a

colorimetric assay of an anthrax biomarker, Anal. Chem. 91 (2019) 12094–12099.
[45] S.M. Han, Y.W. Kim, Y.K. Kim, J.H. Chun, H.B. Oh, S.H. Paek, Performance characterization of two-dimensional paper chromatography-based biosensors for biodefense, exemplified by detection of Bacillus anthracis spores, BioChip J. 12 (2018) 59–68.
[46] D.B. Wang, B. Tian, Z.P. Zhang, X.Y. Wang, J. Fleming, L.J. Bi, R.F. Yang, X. E. Zhang, Detection of Bacillus anthracis spores by super-paramagnetic lateral-flow immunoassays based on "Road Closure,", Biosens. Bioelectron. 67 (2015) 608–614.
[47] L. Upadhyay, V.K. Chaturvedi, P.K. Gupta, S.C. Sunita, T.G. Sumithra, B.R. Prusty, A.K. Yadav, Development of a visible loop mediated isothermal amplification assay for rapid detection of Bacillus anthracis, Biologicals 69 (2021) 59–65.
[48] Y. Zhang, B. Li, H. Ma, L. Zhang, H. Jiang, H. Song, L. Zhang, Y. Luo, A nanoscaled lanthanide metal–organic framework as a colorimetric fluorescence sensor for dipicolinic acid based on modulating energy transfer, J. Mater. Chem. C 4 (2016) 7294–7301.
[49] W.K. Oh, Y.S. Jeong, J. Song, J. Jang, Fluorescent europium-modified polymer nanoparticles for rapid and sensitive anthrax sensors, Biosens. Bioelectron. 29 (2011) 172–177.
[50] Y. Zhang, B. Li, H. Ma, L. Zhang, Y. Zheng, Rapid and facile ratiometric detection of an anthrax biomarker by regulating energy transfer process in bio-metal-organic framework, Biosens. Bioelectron. 85 (2016) 287–293.
[51] K. Shi, Z. Yang, L. Dong, B. Yu, Dual channel detection for anthrax biomarker dipicolinic acid: the combination of an emission turn on probe and luminescent metal-organic frameworks, Sensor. Actuator. B Chem. 266 (2018) 263–269.
[52] X. Li, J. Zhao, Y. Zhu, B. Wang, X. Wei, Y. Shao, Y. Ma, T. Jiang, Colorimetric and ratiometric fluorescent response for anthrax bio-indicator: a combination of rare earth MOF and rhodamine-derived dye, Spectrochim. Acta Mol. Biomol. Spectrosc. 229 (2020), 117999.
[53] D. Yang, S. Mei, Z. Wen, X. Wei, Z. Cui, B. Yang, C. Wei, Y. Qiu, M. Li, H. Li, W. Zhang, Dual-emission of silicon nanoparticles encapsulated lanthanide-based metal-organic frameworks for ratiometric fluorescence detection of bacterial spores, Microchim. Acta 187 (2020) 1–9.
[54] M. Donmez, H.A. Oktem, M.D. Yilmaz, Ratiometric fluorescence detection of an anthrax biomarker with Eu3+-chelated chitosan biopolymers, Carbohydr. Polym. 180 (2018) 226–230.
[55] N. Gao, Y. Zhang, P. Huang, Z. Xiang, F.Y. Wu, L. Mao, Perturbing tandem energy transfer in luminescent heterobinuclear lanthanide coordination polymer nanoparticles enables real-time monitoring of release of the anthrax biomarker from bacterial spores, Anal. Chem. 90 (2018) 7004–7011.
[56] Z. Zhou, J. Gu, Y. Chen, X. Zhang, H. Wu, X. Qiao, Europium functionalized silicon quantum dots nanomaterials for ratiometric fluorescence detection of Bacillus anthrax biomarker, Spectrochim. Acta Mol. Biomol. Spectrosc. 212 (2019) 88–93.
[57] Q. Zhou, Y. Fang, J. Li, D. Hong, P. Zhu, S. Chen, K. Tan, A design strategy of dual-ratiomentric optical probe based on europium-doped carbon dots for colorimetric and fluorescent visual detection of anthrax biomarker, Talanta 222 (2021), 121548.
[58] N. Ariffin, N.A. Yusof, J. Abdullah, S.F. Abd Rahman, N.H. Ahmad Raston, N. Kusnin, S. Suraiya, Lateral flow immunoassay for naked eye detection of Mycobacterium tuberculosis, J. Sens. 2020 (2020) 1–10.
[59] F.A. Wang, T. Lakshmipriya, S.C. Gopinath, Red spectral shift in sensitive colorimetric detection of tuberculosis by ESAT-6 antigen-antibody Complex: a new strategy with gold nanoparticle, Nanoscale Res. Lett. 13 (2018) 1–8.
[60] E.B. Kim, S.A. Cheon, T.S. Shim, H.J. Kim, T.J. Park, Reliable naked-eye detection of Mycobacterium tuberculosis antigen 85B using gold and copper nanoshell-enhanced immunoblotting techniques, Sensor. Actuator. B Chem. 317 (2020), 128220.
[61] G. Kumar, P.K. Dagur, P.K. Singh, H. Shankar, V.S. Yadav, V.M. Katoch, B. Joshi, Serodiagnostic efficacy of Mycobacterium tuberculosis 30/32-kDa mycolyl transferase complex, ESAT-6, and CFP-10 in patients with active tuberculosis, Arch. Immunol. Ther. Exp. 58 (2010) 57–65.
[62] X. Yue, Y. Huang, Y. Zhang, H. Ouyang, J. Xie, Z. Fu, Mycobacteriophage SWU1-Functionalized magnetic particles for facile bioluminescent detection of Mycobacterium smegmatis, Anal. Chim. Acta 1145 (2021) 17–25.
[63] A. Kozajda, K. Jeżak, A. Kapsa, Airborne Staphylococcus aureus in different environments—a review, Environ. Sci. Pollut. Res. 26 (2019) 34741–34753.
[64] P. Liu, L. Han, F. Wang, V.A. Petrenko, A. Liu, Gold nanoprobe functionalized with specific fusion protein selection from phage display and its application in rapid, selective and sensitive colorimetric biosensing of Staphylococcus aureus, Biosens. Bioelectron. 82 (2016) 195–203.
[65] R. Shahbazi, M. Salouti, B. Amini, A. Jalilvand, E. Naderlou, A. Amini, A. Shams, Highly selective and sensitive detection of Staphylococcus aureus with gold nanoparticle-based core-shell nano biosensor, Mol. Cell. Probes 41 (2018) 8–13.
[66] P. Tiet, K.C. Clark, J.O. McNamara, J.M. Berlin, Colorimetric detection of Staphylococcus aureus contaminated solutions without purification, Bioconjugate Chem. 28 (2017) 183–193.
[67] S. Yao, J. Li, B. Pang, X. Wang, Y. Shi, X. Song, K. Xu, J. Wang, C. Zhao, Colorimetric immunoassay for rapid detection of Staphylococcus aureus based on etching-enhanced peroxidase-like catalytic activity of gold nanoparticles, Microchim. Acta 187 (2020) 1–8.
[68] H. Zhang, S. Yao, X. Song, K. Xu, J. Wang, J. Li, C. Zhao, M. Jin, One-step colorimetric detection of Staphylococcus aureus based on target-induced shielding against the peroxidase mimicking activity of aptamer-functionalized gold-coated iron oxide nanocomposites, Talanta 232 (2021), 122448.
[69] A.B. Pebdeni, M. Hosseini, Fast and selective whole cell detection of Staphylococcus aureus bacteria in food samples by paper based colorimetric nanobiosensor using peroxidase-like catalytic activity of DNA-Au/Pt bimetallic nanoclusters, Microchem. J. 159 (2020), 105475.
[70] Y. Li, J. Wang, S. Wang, J. Wang, Rolling circle amplification based colorimetric determination of Staphylococcus aureus, Microchim. Acta 187 (2020) 1–10.
[71] S. Yao, C. Zhao, Y. Liu, H. Nie, G. Xi, X. Cao, Z. Li, B. Pang, J. Li, J. Wang, Colorimetric immunoassay for the detection of Staphylococcus aureus by using magnetic carbon dots and sliver nanoclusters as o-phenylenediamine-oxidase mimetics, Food Anal. Methods 13 (2020) 833–838.
[72] S. Eissa, M. Zourob, A dual electrochemical/colorimetric magnetic nanoparticle/peptide-based platform for the detection of Staphylococcus aureus, Analyst 145 (2020) 4606–4614.
[73] W. Deng, C. Cheng, H. Yang, H. Wang, Y. Tan, Q. Xie, M. Ma, S. Yao, Ultrasensitive immunoassay of Staphylococcus aureus based on colorimetric and fluorescent responses of 4-chloro-7-nitrobenzo-2-oxa-1, 3-diazole to l-cysteine, Talanta 202 (2019) 244–250.
[74] A.B. Pebdeni, M. Mousavizadegan, M. Hosseini, Sensitive detection of S. Aureus using aptamer-and vancomycin-copper nanoclusters as dual recognition strategy, Food Chem. 361 (2021), 130137.
[75] D.H. Enghol, M. Kilian, D.S. Goodsell, E.S. Andersen, R.S. Kjærgaard, A visual review of the human pathogen Streptococcus pneumoniae, FEMS Microbiol. Rev. 41 (2017) 854–879.
[76] W. Chen, Y. Yan, Y. Zhang, X. Zhang, Y. Yin, S. Ding, DNA transducer-triggered signal switch for visual colorimetric bioanalysis, Sci. Rep. 5 (2015) 1–9.
[77] Y. Wang, Y. Wang, D. Li, J. Xu, C. Ye, Detection of nucleic acids and elimination of carryover contamination by using loop-mediated isothermal amplification and antarctic thermal sensitive uracil-DNA-glycosylase in a lateral flow biosensor: application to the detection of Streptococcus pneumoniae, Microchim. Acta 185 (2018) 1–11.
[78] X. Weng, S. Neethirajan, A microfluidic biosensor using graphene oxide and aptamer-functionalized quantum dots for peanut allergen detection, Biosens. Bioelectron. 85 (2016) 649–656.
[79] C. Chen, Z. Zou, L. Chen, X. Ji, Z. He, Functionalized magnetic microparticle-based colorimetric platform for influenza A virus detection, Nanotechnology 27 (2016), 435102.
[80] J. Lee, M. Morita, K. Takemura, E.Y. Park, A multi-functional gold/iron-oxide nanoparticle-CNT hybrid nanomaterial as virus DNA sensing platform, Biosens. Bioelectron. 102 (2018) 425–431.
[81] S.R. Ahmed, J. Kim, T. Suzuki, J. Lee, E.Y. Park, Detection of influenza virus using peroxidase-mimic of gold nanoparticles, Biotechnol. Bioeng. 113 (2016) 2298–2303.
[82] S. Song, K. Ha, K. Guk, S.G. Hwang, J.M. Choi, T. Kang, P. Bae, J. Jung, E.K. Lim, Colorimetric detection of influenza A (H1N1) virus by a peptide-functionalized polydiacetylene (PEP-PDA) nanosensor, RSC Adv. 6 (2016) 48566–48570.
[83] S.U. Son, S.B. Seo, S. Jang, J. Choi, J.W. Lim, D.K. Lee, H. Kim, S. Seo, T. Kang, J. Jung, E.K. Lim, Naked-eye detection of pandemic influenza a (pH1N1) virus by polydiacetylene (PDA)-based paper sensor as a point-of-care diagnostic platform, Sensor. Actuator. B Chem. 291 (2019) 257–265.
[84] Y.D. Ma, Y.S. Chen, G.B. Lee, An integrated self-driven microfluidic device for rapid detection of the influenza A (H1N1) virus by reverse transcription loop-mediated isothermal amplification, Sensor. Actuator. B Chem. 296 (2019), 126647.
[85] O.J. Achadu, K. Takemura, I.M. Khoris, E.Y. Park, Plasmonic/magnetic molybdenum trioxide and graphitic carbon nitride quantum dots-based fluoroimmunosensing system for influenza virus, Sensor. Actuator. B Chem. 321 (2020), 128494.
[86] C.H. Zhou, J.Y. Zhao, D.W. Pang, Z.L. Zhang, Enzyme-induced metallization as a signal amplification strategy for highly sensitive colorimetric detection of avian influenza virus particles, Anal. Chem. 86 (2014) 2752–2759.
[87] H. Zhang, X. Ma, S. Hu, Y. Lin, L. Guo, B. Qiu, Z. Lin, G. Chen, Highly sensitive visual detection of Avian Influenza A (H7N9) virus based on the enzyme-induced metallization, Biosens. Bioelectron. 79 (2016) 874–880.
[88] S. Xu, W. Ouyang, P. Xie, Y. Lin, B. Qiu, Z. Lin, G. Chen, L. Guo, Highly uniform gold nanobipyramids for ultrasensitive colorimetric detection of influenza virus, Anal. Chem. 89 (2017) 1617–1623.
[89] W. Chen, H. Yu, F. Sun, A. Ornob, R. Brisbin, A. Ganguli, V. Vemuri, P. Strzebonski, G. Cui, K.J. Allen, S.A. Desai, Mobile platform for multiplexed detection and differentiation of disease-specific nucleic acid sequences, using microfluidic loop-mediated isothermal amplification and smartphone detection, Anal. Chem. 89 (2017) 11219–11226.
[90] Z. Wu, T. Zeng, W.J. Guo, Y.Y. Bai, D.W. Pang, Z.L. Zhang, Digital single virus immunoassay for ultrasensitive multiplex avian influenza virus detection based on fluorescent magnetic multifunctional nanospheres, ACS Appl. Mater. Interfaces 11 (2019) 5762–5770.
[91] X. Peng, G. Luo, Z. Wu, W. Wen, X. Zhang, S. Wang, Fluorescent-magnetic-catalytic nanospheres for dual-modality detection of H9N2 avian influenza virus, ACS Appl. Mater. Interfaces 11 (2019) 41148–41156.
[92] F. Luo, C. Long, Z. Wu, H. Xiong, M. Chen, X. Zhang, W. Wen, S. Wang, Functional silica nanospheres for sensitive detection of H9N2 avian influenza virus based on immunomagnetic separation, Sensor. Actuator. B Chem. 310 (2020), 127831.
[93] B.S. Batule, S.U. Kim, H. Mun, C. Choi, W.B. Shim, M.G. Kim, Colorimetric detection of norovirus in oyster samples through DNAzyme as a signaling probe, J. Agric. Food Chem. 66 (2018) 3003–3008.
[94] F. Nasrin, A.D. Chowdhury, K. Takemura, J. Lee, O. Adegoke, V.K. Deo, F. Abe, T. Suzuki, E.Y. Park, Single-step detection of norovirus tuning localized surface

plasmon resonance-induced optical signal between gold nanoparticles and quantum dots, Biosens. Bioelectron. 122 (2018) 16–24.
[95] I.M. Khoris, K. Takemura, J. Lee, T. Hara, F. Abe, T. Suzuki, E.Y. Park, Enhanced colorimetric detection of norovirus using in-situ growth of Ag shell on Au NPs, Biosens. Bioelectron. 126 (2019) 425–432.
[96] H.A. Alhadrami, S. Al-Amer, Y. Aloraij, F. Alhamlan, R. Chinnappan, K.M. Abu-Salah, S. Almatrrouk, M.M. Zourob, Development of a simple, fast, and cost-effective nanobased immunoassay method for detecting Norovirus in food samples, ACS Omega 5 (2020) 12162–12165.
[97] S.R. Ahmed, K. Takemeura, T.C. Li, N. Kitamoto, T. Tanaka, T. Suzuki, E.Y. Park, Size-controlled preparation of peroxidase-like graphene-gold nanoparticle hybrids for the visible detection of norovirus-like particles, Biosens. Bioelectron. 87 (2017) 558–565.
[98] A.B. Ganganboina, A.D. Chowdhury, I.M. Khoris, F. Nasrin, K. Takemura, T. Hara, F. Abe, T. Suzuki, E.Y. Park, Dual modality sensor using liposome-based signal amplification technique for ultrasensitive norovirus detection, Biosens. Bioelectron. 157 (2020), 112169.
[99] X. Weng, S. Neethirajan, Aptamer-based fluorometric determination of norovirus using a paper-based microfluidic device, Microchim. Acta 184 (2017) 4545–4552.
[100] K. Takemura, J. Lee, T. Suzuki, T. Hara, F. Abe, E.Y. Park, Ultrasensitive detection of norovirus using a magnetofluoroimmunoassay based on synergic properties of gold/magnetic nanoparticle hybrid nanocomposites and quantum dots, Sensor. Actuator. B Chem. 296 (2019), 126672.
[101] F. Shen, Y. Cheng, Y. Xie, H. Yu, W. Yao, H.W. Li, Y. Guo, H. Qian, DNA-silver nanocluster probe for norovirus RNA detection based on changes in secondary structure of nucleic acids, Anal. Biochem. 583 (2019), 113365.
[102] A.D. Chowdhury, S. Sharmin, F. Nasrin, M. Yamazaki, F. Abe, T. Suzuki, E. Y. Park, Use of target-specific liposome and magnetic nanoparticle conjugation for the amplified detection of norovirus, ACS Appl. Bio Mater. 3 (2020) 3560–3568.
[103] G. Chellasamy, S.K. Arumugasamy, S. Govindaraju, K. Yun, Analytical insights of COVID-19 pandemic, Trends Anal. Chem. 133 (2020), 116072.
[104] A. Karami, M. Hasani, F.A. Jalilian, R. Ezati, Conventional PCR assisted single-component assembly of spherical nucleic acids for simple colorimetric detection of SARS-CoV-2, Sensor. Actuator. B Chem. 328 (2021), 128971.
[105] M. Alafeef, P. Moitra, K. Dighe, D. Pan, RNA-extraction-free nano-amplified colorimetric test for point-of-care clinical diagnosis of COVID-19, Nat. Protoc. 16 (2021) 3141–3162.
[106] P. Moitra, M. Alafeef, K. Dighe, M.B. Frieman, D. Pan, Selective naked-eye detection of SARS-CoV-2 mediated by N gene targeted antisense oligonucleotide capped plasmonic nanoparticles, ACS Nano 14 (2020) 7617–7627.
[107] S.B. Moon, J.H. Ko, Y.S. Kim, Recent advances in the CRISPR genome editing tool set, Exp. Mol. Med. 51 (2019) 1–11.
[108] J. Moon, H.J. Kwon, D. Yong, I.C. Lee, H. Kim, H. Kang, E.K. Lim, K.S. Lee, J. Jung, H.G. Park, T. Kang, Colorimetric detection of sars-cov-2 and drug-resistant ph1n1 using crispr/dcas9, ACS Sens. 5 (2020) 4017–4026.
[109] A. Roda, S. Cavalera, F. Di Nardo, D. Calabria, S. Rosati, P. Simoni, B. Colitti, C. Baggiani, M. Roda, L. Anfossi, Dual lateral flow optical/chemiluminescence immunosensors for the rapid detection of salivary and serum IgA in patients with COVID-19 disease, Biosens. Bioelectron. 172 (2021), 112765.
[110] D. Liu, C. Ju, C. Han, R. Shi, X. Chen, D. Duan, J. Yan, X. Yan, Nanozyme chemiluminescence paper test for rapid and sensitive detection of SARS-CoV-2 antigen, Biosens. Bioelectron. 173 (2021), 112817.
[111] R. Das, A.K. Goel, M.K. Sharma, S. Upadhyay, Electrochemical DNA sensor for anthrax toxin activator gene atxA-detection of PCR amplicons, Biosens. Bioelectron. 74 (2015) 939–946.
[112] D.F. Waller, B.E. Hew, C. Holdaway, M. Jen, G.D. Peckham, Rapid detection of Bacillus anthracis spores using immunomagnetic separation and amperometry, Biosensors 6 (2016) 61.
[113] V. Mazzaracchio, D. Neagu, A. Porchetta, E. Marcoccio, A. Pomponi, G. Faggioni, N. D'Amore, A. Notargiacomo, M. Pea, D. Moscone, G. Palleschi, A label-free impedimetric aptasensor for the detection of Bacillus anthracis spore simulant, Biosens. Bioelectron. 126 (2019) 640–646.
[114] M.K. Sharma, J. Narayanan, S. Upadhyay, A.K. Goel, Electrochemical immunosensor based on bismuth nanocomposite film and cadmium ions functionalized titanium phosphates for the detection of anthrax protective antigen toxin, Biosens. Bioelectron. 74 (2015) 299–304.
[115] I. Magrina, M. Jauset-Rubio, M. Ortiz, H. Tomaso, A. Simonova, M. Hocek, C. K. O'Sullivan, Duplex electrochemical DNA sensor to detect bacillus anthracis CAP and PAG DNA targets based on the incorporation of tailed primers and ferrocene-labeled dATP, ACS Omega 4 (2019) 21900–21908.
[116] M.K. Sharma, J. Narayanan, D. Pardasani, D.N. Srivastava, S. Upadhyay, A. K. Goel, Ultrasensitive electrochemical immunoassay for surface array protein, a Bacillus anthracis biomarker using Au–Pd nanocrystals loaded on boron-nitride nanosheets as catalytic labels, Biosens. Bioelectron. 80 (2016) 442–449.
[117] S.R. Torati, V. Reddy, S.S. Yoon, C. Kim, Electrochemical biosensor for Mycobacterium tuberculosis DNA detection based on gold nanotubes array electrode platform, Biosens. Bioelectron. 78 (2016) 483–488.
[118] M.H.M. Zaid, J. Abdullah, N.A. Yusof, Y. Sulaiman, H. Wasoh, M.F.M. Noh, R. Issa, PNA biosensor based on reduced graphene oxide/water soluble quantum dots for the detection of Mycobacterium tuberculosis, Sensor. Actuator. B Chem. 241 (2017) 1024–1034.
[119] S. Bizid, S. Blili, R. Mlika, A.H. Said, H. Korri-Youssoufi, Direct Electrochemical DNA Sensor based on a new redox oligomer modified with ferrocene and carboxylic acid: application to the detection of Mycobacterium Tuberculosis mutant strain, Anal. Chim. Acta 994 (2017) 10–18.
[120] K.S. Rizi, B. Hatamluyi, M. Rezayi, Z. Meshkat, M. Sankian, K. Ghazvini, H. Farsiani, E. Aryan, Response surface methodology optimized electrochemical DNA biosensor based on HAPNPTs/PPY/MWCNTs nanocomposite for detecting Mycobacterium tuberculosis, Talanta 226 (2021), 122099.
[121] M. Sypabekova, P. Jolly, P. Estrela, D. Kanayeva, Electrochemical aptasensor using optimized surface chemistry for the detection of Mycobacterium tuberculosis secreted protein MPT64 in human serum, Biosens. Bioelectron. 123 (2019) 141–151.
[122] L. Bai, Y. Chen, Y. Bai, Y. Chen, J. Zhou, A. Huang, Fullerene-doped polyaniline as new redox nanoprobe and catalyst in electrochemical aptasensor for ultrasensitive detection of Mycobacterium tuberculosis MPT64 antigen in human serum, Biomaterials 133 (2017) 11–19.
[123] Y. Chen, X. Liu, S. Guo, J. Cao, J. Zhou, J. Zuo, L. Bai, A sandwich-type electrochemical aptasensor for Mycobacterium tuberculosis MPT64 antigen detection using C60NPs decorated N-CNTs/GO nanocomposite coupled with conductive PEI-functionalized metal-organic framework, Biomaterials 216 (2019), 119253.
[124] L. Bai, Y. Chen, X. Liu, J. Zhou, J. Cao, L. Hou, S. Guo, Ultrasensitive electrochemical detection of Mycobacterium tuberculosis IS6110 fragment using gold nanoparticles decorated fullerene nanoparticles/nitrogen-doped graphene nanosheet as signal tags, Anal. Chim. Acta 1080 (2019) 75–83.
[125] P. Eloi, G.A. Nascimento, C. Córdula, V. Visani, H. Castelletti, G. Bezerra, L. Soares, B. Lima, D. Bruneska, L.M.L. Montenegro, H.C. Schindler, Toward a point-of-care diagnostic for specific detection of Mycobacterium tuberculosis from sputum samples, Tuberculosis 121 (2020), 101919.
[126] P. Yuanfeng, L. Ruiyi, X. Qingqing, C. Xiaofen, Y. Yongqiang, L. Zaijun, Electrochemical detection of Mycobacterium tuberculosis IS6110 gene fragments based on the gold nanocrystals with uniform morphology and highly exposed high-index facets and target DNA-induced recycling amplification, Sensor. Actuator. B Chem. 314 (2020), 128061.
[127] Y. Chen, S. Guo, M. Zhao, P. Zhang, Z. Xin, J. Tao, L. Bai, Amperometric DNA biosensor for Mycobacterium tuberculosis detection using flower-like carbon nanotubes-polyaniline nanohybrid and enzyme-assisted signal amplification strategy, Biosens. Bioelectron. 119 (2018) 215–220.
[128] U.Z. Mohd Azmi, N.A. Yusof, N. Kusnin, J. Abdullah, S. Suraiya, P.S. Ong, N. H. Ahmad Raston, S.F. Abd Rahman, M.F. Mohamad Fathil, Sandwich electrochemical immunosensor for early detection of tuberculosis based on graphene/polyaniline-modified screen-printed gold electrode, Sensors 18 (2018) 3926.
[129] J. Kim, M. Jang, K.G. Lee, K.S. Lee, S.J. Lee, K.W. Ro, J. Lee, Plastic-chip-based magnetophoretic immunoassay for point-of-care diagnosis of tuberculosis, ACS Appl. Mater. Interfaces 8 (2016) 23489–23497.
[130] L.T. Tufa, S. Oh, J. Kim, K.J. Jeong, T.J. Park, H.J. Kim, J. Lee, Electrochemical immunosensor using nanotriplex of graphene quantum dots, Fe3O4, and Ag nanoparticles for tuberculosis, Electrochim. Acta 290 (2018) 369–377.
[131] N.M. Bakhori, N.A. Yusof, J. Abdullah, H. Wasoh, S.K. Ab Rahman, S.F. Abd Rahman, Surface enhanced CdSe/ZnS QD/SiNP electrochemical immunosensor for the detection of Mycobacterium tuberculosis by combination of CFP10-ESAT6 for better diagnostic specificity, Materials 13 (2020) 149.
[132] W. Sun, X. Wang, W. Wang, Y. Lu, J. Xi, W. Zheng, F. Wu, H. Ao, G. Li, Electrochemical DNA sensor for Staphylococcus aureus nuc gene sequence with zirconia and graphene modified electrode, J. Solid State Electrochem. 19 (2015) 2431–2438.
[133] A. Mathur, R. Gupta, S. Kondal, S. Wadhwa, R.N. Pudake, R. Kansal, C.S. Pundir, J. Narang, A new tactics for the detection of S. aureus via paper based geno-interface incorporated with graphene nano dots and zeolites, Int. J. Biol. Macromol. 112 (2018) 364–370.
[134] J. Bhardwaj, S. Devarakonda, S. Kumar, J. Jang, Development of a paper-based electrochemical immunosensor using an antibody-single walled carbon nanotubes bio-conjugate modified electrode for label-free detection of foodborne pathogens, Sensor. Actuator. B Chem. 253 (2017) 115–123.
[135] H. Wang, Y. Xiu, Y. Chen, L. Sun, L. Yang, H. Chen, X. Niu, Electrochemical immunosensor based on an antibody-hierarchical mesoporous SiO 2 for the detection of Staphylococcus aureus, RSC Adv. 9 (2019) 16278–16287.
[136] E. Han, X. Li, Y. Zhang, M. Zhang, J. Cai, X. Zhang, Electrochemical immunosensor based on self-assembled gold nanorods for label-free and sensitive determination of Staphylococcus aureus, Anal. Biochem. 611 (2020), 113982.
[137] H. Wang, X. Zhao, H. Yang, L. Cao, W. Deng, Y. Tan, Q. Xie, Three-dimensional macroporous gold electrodes superior to conventional gold disk electrodes in the construction of an electrochemical immunobiosensor for Staphylococcus aureus detection, Analyst 145 (2020) 2988–2994.
[138] U. Farooq, M.W. Ullah, Q. Yang, A. Aziz, J. Xu, L. Zhou, S. Wang, High-density phage particles immobilization in surface-modified bacterial cellulose for ultra-sensitive and selective electrochemical detection of Staphylococcus aureus, Biosens. Bioelectron. 157 (2020), 112163.
[139] R. Cai, S. Zhang, L. Chen, M. Li, Y. Zhang, N. Zhou, Self-assembled DNA nanoflowers triggered by a DNA walker for highly sensitive electrochemical detection of Staphylococcus aureus, ACS Appl. Mater. Interfaces 13 (2021) 4905–4914.
[140] R. Cai, Z. Zhang, H. Chen, Y. Tian, N. Zhou, A versatile signal-on electrochemical biosensor for Staphylococcus aureus based on triple-helix molecular switch, Sensor. Actuator. B Chem. 326 (2021), 128842.
[141] F. Li, Z. Yu, Y. Xu, H. Ma, G. Zhang, Y. Song, H. Yan, X. He, Using the synergism strategy for highly sensitive and specific electrochemical sensing of Streptococcus pneumoniae Lyt-1 gene sequence, Anal. Chim. Acta 886 (2015) 175–181.

[142] A.S. Afonso, L.R. Goulart, I.M. Goulart, A.E. Machado, J.M. Madurro, A.G. Brito-Madurro, A promising bioelectrode based on gene of Mycobacterium leprae immobilized onto poly (4-aminophenol), J. Appl. Polym. Sci. 118 (2010) 2921–2928.
[143] F.P. Ferreira, A.C. Honorato-Castro, J.V. da Silva, S.C. Orellana, G.C. Oliveira, J. M. Madurro, A.G. Brito-Madurro, A novel polymer-based genosensor for the detection and quantification of Streptococcus pneumoniae in genomic DNA sample, Polym. Eng. Sci. 58 (2018) 1308–1314.
[144] J. Wang, M.C. Leong, E.Z.W. Leong, W.S. Kuan, D.T. Leong, Clinically relevant detection of Streptococcus pneumoniae with DNA-antibody nanostructures, Anal. Chem. 89 (2017) 6900–6906.
[145] X. Cui, A. Das, A.N. Dhawane, J. Sweeney, X. Zhang, V. Chivukula, S.S. Iyer, Highly specific and rapid glycan based amperometric detection of influenza viruses, Chem. Sci. 8 (2017) 3628–3634.
[146] T. Matsubara, M. Ujie, T. Yamamoto, M. Akahori, Y. Einaga, T. Sato, Highly sensitive detection of influenza virus by boron-doped diamond electrode terminated with sialic acid-mimic peptide, Proc. Natl. Acad. Sci. U. S. A 113 (2016) 8981–8984.
[147] D. Nidzworski, K. Siuzdak, P. Niedziałkowski, R. Bogdanowicz, M. Sobaszek, J. Ryl, P. Weiher, M. Sawczak, E. Wnuk, W.A. Goddard, A. Jaramillo-Botero, A rapid-response ultrasensitive biosensor for influenza virus detection using antibody modified boron-doped diamond, Sci. Rep. 7 (2017) 1–10.
[148] S.R. Joshi, A. Sharma, G.H. Kim, J. Jang, Low cost synthesis of reduced graphene oxide using biopolymer for influenza virus sensor, Mater. Sci. Eng. C 108 (2020), 110465.
[149] A. Dalal Ravina, P.S. Gill, J. Narang, M. Prasad, H. Mohan, Genosensor for rapid, sensitive, specific point-of-care detection of H1N1 influenza (swine flu), Process Biochem. 98 (2020) 262–268.
[150] K. Takemura, A.B. Ganganboina, I.M. Khoris, A.D. Chowdhury, E.Y. Park, Plasmon nanocomposite-enhanced optical and electrochemical signals for sensitive virus detection, ACS Sens. 6 (2021) 2605–2612.
[151] R. Singh, S. Hong, J. Jang, Label-free detection of influenza viruses using a reduced graphene oxide-based electrochemical immunosensor integrated with a microfluidic platform, Sci. Rep. 7 (2017) 1–11.
[152] H.O. Kaya, A.E. Cetin, M. Azimzadeh, S.N. Topkaya, Pathogen detection with electrochemical biosensors: advantages, challenges and future perspectives, J. Electroanal. Chem. 882 (2021), 114989.
[153] J. Lin, R. Wang, P. Jiao, Y. Li, Y. Li, M. Liao, Y. Yu, M. Wang, An impedance immunosensor based on low-cost microelectrodes and specific monoclonal antibodies for rapid detection of avian influenza virus H5N1 in chicken swabs, Biosens. Bioelectron. 67 (2015) 546–552.
[154] J. Lum, R. Wang, B. Hargis, S. Tung, W. Bottje, H. Lu, Y. Li, An impedance aptasensor with microfluidic chips for specific detection of H5N1 avian influenza virus, Sensors 15 (2015) 18565–18578.
[155] S. Karash, R. Wang, L. Kelso, H. Lu, T.J. Huang, Y. Li, Rapid detection of avian influenza virus H5N1 in chicken tracheal samples using an impedance aptasensor with gold nanoparticles for signal amplification, J. Virol. Methods 236 (2016) 147–156.
[156] T. Lee, S.Y. Park, H. Jang, G.H. Kim, Y. Lee, C. Park, M. Mohammadniaei, M. H. Lee, J. Min, Fabrication of electrochemical biosensor consisted of multi-functional DNA structure/porous au nanoparticle for avian influenza virus (H5N1) in chicken serum, Mater. Sci. Eng. C 99 (2019) 511–519.
[157] J.H. Han, D. Lee, C.H.C. Chew, T. Kim, J.J. Pak, A multi-virus detectable microfluidic electrochemical immunosensor for simultaneous detection of H1N1, H5N1, and H7N9 virus using ZnO nanorods for sensitivity enhancement, Sensor. Actuator. B Chem. 228 (2016) 36–42.
[158] H.J. Hwang, M.Y. Ryu, C.Y. Park, J. Ahn, H.G. Park, C. Choi, S.D. Ha, T.J. Park, J. P. Park, High sensitive and selective electrochemical biosensor: label-free detection of human norovirus using affinity peptide as molecular binder, Biosens. Bioelectron. 87 (2017) 164–170.
[159] S.H. Baek, M.W. Kim, C.Y. Park, C.S. Choi, S.K. Kailasa, J.P. Park, T.J. Park, Development of a rapid and sensitive electrochemical biosensor for detection of human norovirus via novel specific binding peptides, Biosens. Bioelectron. 123 (2019) 223–229.
[160] L. Wang, Q. Xiong, F. Xiao, H. Duan, 2D nanomaterials based electrochemical biosensors for cancer diagnosis, Biosens. Bioelectron. 89 (2017) 136–151.
[161] S.H. Baek, C.Y. Park, T.P. Nguyen, M.W. Kim, J.P. Park, C. Choi, S.Y. Kim, S. K. Kailasa, T.J. Park, Novel peptides functionalized gold nanoparticles decorated tungsten disulfide nanoflowers as the electrochemical sensing platforms for the norovirus in an oyster, Food Control 114 (2020), 107225.
[162] S.A. Hong, J. Kwon, D. Kim, S. Yang, A rapid, sensitive and selective electrochemical biosensor with concanavalin A for the preemptive detection of norovirus, Biosens. Bioelectron. 64 (2015) 338–344.
[163] J. Lee, K. Takemura, C.N. Kato, T. Suzuki, E.Y. Park, Binary nanoparticle graphene hybrid structure-based highly sensitive biosensing platform for norovirus-like particle detection, ACS Appl. Mater. Interfaces 9 (2017) 27298–27304.
[164] W.A. El-Said, A.S. Al-Bogami, W. Alshitari, D.A. El-Hady, T.S. Saleh, El-Mokhtar M.A., J.W. Choi, Electrochemical Microbiosensor for Detecting COVID-19 in a Patient Sample Based on Gold Microcuboids Pattern, Biochip J. 15 (2021) 287–295.
[165] S.S. Mahshid, S.E. Flynn, S. Mahshid, The potential application of electrochemical biosensors in the COVID-19 pandemic: a perspective on the rapid diagnostics of SARS-CoV-2, Biosens. Bioelectron. 176 (2021), 112905.
[166] M.Z. Rashed, J.A. Kopechek, M.C. Priddy, K.T. Hamorsky, K.E. Palmer, N. Mittal, J. Valdez, J. Flynn, S.J. Williams, Rapid detection of SARS-CoV-2 antibodies using electrochemical impedance-based detector, Biosens. Bioelectron. 171 (2021), 112709.
[167] B.S. Vadlamani, T. Uppal, S.C. Verma, M. Misra, Functionalized TiO2 nanotube-based electrochemical biosensor for rapid detection of SARS-CoV-2, Sensors 20 (2020) 5871.
[168] B. Mojsoska, S. Larsen, D.A. Olsen, J.S. Madsen, I. Brandslund, F.A. Alatraktchi, Rapid SARS-CoV-2 detection using electrochemical immunosensor, Sensors 21 (2021) 390.
[169] J. Tian, Z. Liang, O. Hu, Q. He, D. Sun, Z. Chen, An electrochemical dual-aptamer biosensor based on metal-organic frameworks MIL-53 decorated with Au@ Pt nanoparticles and enzymes for detection of COVID-19 nucleocapsid protein, Electrochim. Acta 387 (2021), 138553.
[170] H. Zhao, F. Liu, W. Xie, T.C. Zhou, J. OuYang, L. Jin, H. Li, C.Y. Zhao, L. Zhang, J. Wei, Y.P. Zhang, Ultrasensitive supersandwich-type electrochemical sensor for SARS-CoV-2 from the infected COVID-19 patients using a smartphone, Sensor. Actuator. B Chem. 327 (2021), 128899.
[171] H.E. Kim, A. Schuck, S.H. Lee, Y. Lee, M. Kang, Y.S. Kim, Sensitive electrochemical biosensor combined with isothermal amplification for point-of-care COVID-19 tests, Biosens. Bioelectron. 182 (2021), 113168.

Doctor Rajamanickam Sivakumar received a Ph.D from Annamalai University, India and conducted postdoctoral research at Inha University, South Korea. In 2019, he joined as an Assistant Professor at Gachon University, South Korea. His major research direction lies in biosensors fabrication, colorimetric nucleic acid detection, and microfluidics.

Professor Nae Yoon Lee received a Ph.D from the University of Tokyo in 2004 and worked as a postdoctoral fellow in Korea Advanced Institute of Science and Technology (KAIST) and as a research professor at Ewha Womans University in South Korea from 2004 to 2007. She is currently a Professor in the Department of BioNano Technology at Gachon University since 2007. Her main research field is concerned with the development of Lab-on-a-Chip system particularly focusing on micro-device fabrication and sealing, surface modification, and developing portable diagnostic devices for point-of-care testing (POCT).